INTERLEUKIN-1β DRIVES PROSTATE CANCER CELL COOPERATION IN THE BONE METASTATIC NICHE

by

Kristina S. Shahriari

August 2016

A Dissertation Presented to the Faculty of
Drexel University College of Medicine
in partial fulfillment of the Requirements for the Degree of
Doctor of Philosophy

Olimpia Meucci, M.D., Ph.D.
Professor and Chair
Department of Pharmacology and Physiology

Alessandro Fatatis, M.D., Ph.D.
Professor
Department of Pharmacology and Physiology

Paul Campbell, Ph.D.
Assistant Professor
Department of Pharmacology and Physiology

Bradford Jameson, Ph.D.
Professor
Department of Biochemistry and Molecular Biology

Edna Cukierman, Ph.D.
Professor and Chair
Department of Cancer Biology
Fox Chase Cancer Center

For my father, Dr. Ali A. Shahriari.

ACKNOWLEDGEMENTS

The work that follows depended on the help of more people than can be reasonably listed here, but I will do my best.

Thanks to my advisor, Alessandro Fatatis, who always found an hour or four to talk with me; a mentor in the truest sense.

To my fellow lab members, past and present, most especially Danielle Jernigan, Qingxin "Cindy" Liu, and Fei Shen; I would have been lost without their patience and generosity.

To my committee members, Paul Campbell, Bradford Jameson, Eti Cukierman, and especially my chair, Olimpia Meucci: they have supported me and this work through one of the most trying times in my life, and without them this dissertation would not be.

To the Department of Pharmacology and Physiology, and all the people who made it a joyful, invigorating environment in which to do science.

And finally, to my family: Mama, Sara, David, and especially Dickie, for the millions of little things they've done so that I could be where I am today.

TABLE OF CONTENTS

LIST OF TABLES

LIST OF ILLUSTRATIONS

Figure 13: The fraction of prostate cancer cells negative for AR expression detected in bone metastases from ten CRPC patients was found to be 33±14%, with the percentage of infiltrating or resident non-cancerous cells (immune, endothelial or stromal origin) not exceeding 1-2%. Each dot indicates a unique microscopic field of view in which cells were counted.

Figure 14: Primary (*left*) and bone metastatic (*right*) tissues stained for pan-cytokeratin (green) and AR (red), with nuclei in blue. These representative images show that both AR+ (red nuclei) and AR− (blue nuclei) cancer cells are of epithelial-derived, and are present in the basal compartment of primary tumors as well as mixed with AR+ cells in skeletal metastases (yellow arrows). Non-epithelial AR− cells were identified in the bone marrow stroma (green arrows).

Figure 15: Molecular analysis of tumor and stromal components of human skeletal metastases from prostate cancer patients: tissue samples from areas of tumors lacking (*top*) or highly positive (*middle*) for AR were collected by laser-capture microdissection, as was normal stromal tissue located away from tumor (*bottom*).

Figure 16: Molecular analysis of tumor and stromal components of human skeletal metastases from prostate cancer patients: qRT-PCR was used to evaluate the expression of the prostate-specific marker prostein, which was detected at comparable levels in prostate cancer cells independently of their AR status, indicating the prostatic origin of both these populations (*left*). The lack of AR expression in cells that stained negative by immunohistochemistry was confirmed at the transcriptional level, providing the first molecular evidence for AR− prostate cancer cells in human skeletal metastases (*right*).

Figure 17: Specimen from a lung metastasis biopsy in a patient with advanced prostate adenocarcinoma, stained with Hematoxylin-Eosin (*left*) and for AR (*right*); a positive control for AR staining may be seen in *Fig. 15*. The absence of AR expression seen here is typical of visceral metastases in these patients.

Figure 18: Immunoblot analysis reveals that PC3-ML are the only human prostate cancer cell line tested which endogenously expresses IL-1β.

Figure 19: Molecular analysis of tumor and stromal components of human skeletal metastases from prostate cancer patients: IL-1β mRNA was detected exclusively in AR-negative cancer cells, while considerably lower levels were detected in the bone stroma.

"The knowledge of anything, since all things have causes,
is not acquired or complete unless it is known by its causes."

ibn Sīnā
The Canon of Medicine
circa 1020 CE

ABSTRACT

Interleukin-1β drives prostate cancer cell cooperation
in the bone metastatic niche

Kristina S. Shahriari

Alessandro Fatatis, M.D., Ph.D.

Localized prostate cancer (PCa) is fueled by androgens. The androgen receptor (AR) is also thought to play a vital role in the disseminated castration-resistant form of the disease (CRPC) that primarily affects the skeleton. Here we show that approximately 33% of PCa cells in skeletal metastases lack AR and express high levels of Interleukin-1β (IL-1β), while cells expressing AR were negative for this cytokine.

We previously identified IL-1β as a major mediator of the bone-metastatic behavior of human prostate cancer cells inoculated into the left cardiac ventricle of SCID mice. In this study, AR-/IL-1β+ human PCa cells were found to influence the bone stroma, promoting the development of carcinoma-associated fibroblasts (CAFs). Indeed, mice null for the IL-1 receptor (IL-1R) are much less prone to colonization by AR-/IL-1β+ cancer cells, as are animals treated with the IL-1R antagonist Anakinra. Thus, tumor-derived IL-1β induces the bone stroma to

establish a metastasis-permissive microenvironment. Remarkably, this metastatic niche supports not only AR-/IL-1β+ cells, but also AR+/IL-1β- cancer cells that are otherwise unable to form skeletal tumors: the presence of AR-/IL-1β+ cells allowed AR+/IL-1β- cells both to colonize the bone and to persist and grow into macroscopic mixed tumors. Using molecular analysis of the affected stroma, we have identified multiple factors which may be responsible for this phenomenon and are represent novel therapeutic targets.

We propose that cooperation amongst PCa cells demonstrates a functional role for phenotypic heterogeneity in human bone metastasis. These discoveries may be exploited therapeutically to alter the microenvironment of the metastatic niche, with the aim to impair establishment and progression of bone metastatic disease in patients with CRPC.

Chapter 1: The prostate and its malignancies

The prostate gland

The human prostate is a glandular organ, one of a group of sex accessory tissues which are responsible for composing and conducting semen through the male reproductive tract. The seminal vesicles, prostate, bulbourethral gland, and glands of Littre cooperate to produce seminal plasma, the non-cellular component of semen. Each of these tissues contributes specific elements to the complex fluid responsible for supporting and sustaining spermatozoa upon ejaculation. The prostate secretion itself is chiefly made up of citric acid, acid phosphatases, zinc, and a variety of proteolytic enzymes, with distinct regions of the gland producing the various elements [1].

Anatomically, the prostate resides within the pelvis ventral to the rectum and caudal to the bladder, where it surrounds the urethra and ejaculatory ducts. The organ itself is divided into three glandular zones, the architecture of which is distinct enough to enable differentiation by ultrasound and histology. The central zone comprises about 25% of the gland and encloses both ejaculatory ducts. Ventral to this is the transitional lobe: while only consisting of around 5% of the

prostate, it encircles the urethra and is the most common site of benign prostatic hyperplasia (BPH), leading to many of the urinary problems associated with that condition. Finally, the peripheral zone accounts for the remaining 70-75% of the gland, surrounding the other two regions from the dorsal side [2]. As such, it is the most readily palpable region of the prostate upon digital rectal examination (DRE). This is fortunate, as this zone is the source of the great majority of prostate cancers, which may then be detected through this inexpensive and minimally invasive method [3].

Upon microscopic examination, the normal human prostate is revealed to consist of tubuloalveolar glands encased in a fibromuscular stroma at a 1:2 volumetric ratio [4]. Malignancies of the prostate derive exclusively from the epithelial layer, and as such are classified as adenocarcinoma [3]. The epithelium itself is largely made up of two cell layers: secretory columnar epithelium atop a low cuboidal basal layer. A third population, neuroendocrine cells, exist among the secretory component as a small percentage of the total epithelium, but are thought to have an outsized influence on glandular function. They express the neuroendocrine-specific proteins chromogranin-A and synaptophysin, as well as the neurotransmitter serotonin and various other bioactive molecules which are theorized to influence the proliferation, differentiation, and activity of the surrounding gland. Basal cells of the prostatic epithelium represent less than 10%

of the total cell number and have a low proliferation rate and little secretory activity; while the evidence is not fully conclusive, these cells are understood to be the progenitors of both other epithelial cell types. This suggests that the basal epithelium is the origin of prostatic stem cells, which due to their pluripotent nature are often implicated in the development of prostate adenocarcinoma, particularly in aggressive cases [2, 5].

Epidemiology of prostate cancer

Prostate carcinoma (PCa) is the most prevalent malignancy among American men, with 180,890 new cases and 26,120 deaths due to PCa expected in 2016 [6]. Lifetime mortality risk from PCa among men in the US is 2.71%, making it the second most deadly cancer for males. Among African American men the lifetime mortality risk from PCa rises to 4.55% [7], indicating that effective treatments for PCa will help address a major healthcare disparity in the US.

While 14.0% of American men will develop prostate cancer over their lifetime, the five-year survival rate from 2006-2012 was an impressive 98.9% [6]. This is due to a number of factors, chief among them the indolent character of most cases; current best practices advise against PCa screening for men with a life expectancy of less than ten years, as disease progression is unlikely to significantly impact a person's life over this period of time [8, 9]. Thus a five-year survival rate can be deceiving, as can pooled statistics across a patient population. For instance,

while individuals with organ-confined or locally invasive PCa at diagnosis exhibit a five-year survival rate approaching 100% [6], men with bone metastatic disease have rates as low as 3% [10].

Pathophysiology of prostate cancer

Normal epithelial cells are subject to a number of in-built limitations which, in combination with external influences on both the local and organismal scale, ensure the proper maintenance and function of the tissue in question. For example, the prostatic epithelium exhibits a characteristic bilayer, with columnar secretory cells overlaying the cuboidal basal layer. The luminal cells in this case are terminally differentiated, and therefore cannot further replicate themselves: in order to be replaced, a new secretory cell must be produced by the basal layer via a series of differentiating cell divisions [11]. Additionally, luminal cells like those of the prostate are unable to thrive in the absence of anchorage to underlying matrix; otherwise these cells will undergo anoikis, a specific type of apoptosis which occurs in the absence of cell adhesion. Through these local mechanisms it is apparent that individual normally-functioning cells help maintain overall tissue structure and function [12].

Thus the development of carcinoma requires two fundamental alterations in the behavior of healthy cells: that they become "immortalized," which is to say that they may replicate an unlimited number of times, and "transformed,"

meaning that they can survive and even grow without physical attachment to supportive matrix or stroma. Such cells would be free to proliferate without restraint, eventually filling the glandular lumen with cells in a pre-cancerous lesion known as prostatic intraepithelial neoplasia (PIN). If these cells should penetrate beyond the boundary of the glandular basement membrane, prostate adenocarcinoma has occurred [5].

Cancer cells are frequently resistant to external regulation, often by becoming both impervious to anti-proliferative signals and self-sufficient in matters of growth factors or other proliferative signaling molecules. For instance, normal prostate epithelial cells require androgens in order to survive and multiply, and androgen deprivation therapy is typically used to treat invasive and metastatic PCa. This approach is initially effective in reducing tumor growth and burden, but the selective pressure of a testosterone-free environment enables cell populations to develop which are androgen-independent, either through increased sensitivity to alternate androgens, which may be locally produced, by virtue of mutated androgen receptors which are active even in the absence of ligand, or by eliminating the need for androgens altogether. This results in castration-resistant prostate cancer (CRPC), a disease state which thus far remains incurable [5, 11]. Unfortunately, characteristics that would enable distinction between dangerous cancers which will fatally progress and more indolent, less

worrisome forms have yet to be identified at the level of the primary tumor. This makes risk stratification among patients very difficult for a disease in which the majority of cases will prove to be easily managed, necessitating a vigilant and pragmatic approach to patient care [3].

The dominant form of prostate cancer, accounting for more than 90% of cases, is adenocarcinoma arising from prostate epithelial cells. These tumors typically emerge from the terminal acini and progress through PIN before becoming fully malignant [13]. Although it is understood that prostate acinar cells are the forbearers of such tumors, whether the progenitors are basal or secretory remains unknown. Recent studies have proposed that less-aggressive forms of PCa derive from the terminally differentiated luminal population, while more aggressive disease results from mutated basal cells, benefiting from their pluripotency [14].

A notable type of prostate cancer is the neuroendocrine from. This disease may result either from malignant transformation of the resident prostatic neuroendocrine cells, or from cellular transdifferentiation within more typical PCa. Pure neuroendocrine tumors are rare, representing less than 1% of total prostate cancer, but up to half of prostate adenocarcinomas are positive for multiple neuroendocrine markers by immunohistochemistry [13]. Neuroendocrine components to PCa are worrisome because they are associated

with soft tissue metastasis and poor prognosis. However, the multifarious nature of most neuroendocrine prostate tumors make it difficult to determine the causal roles each cell type may play; thus, a neuroendocrine contribution must be considered when developing a clinical approach to PCa [15].

Prostate cancer progression

As with many malignancies, primary prostate cancer alone is almost never fatal, while metastasis is incurable. Thus, the ability to assess and define the degree of PCa progression is of vital importance to effective management of the disease.

In the case of solid tumors, progression is generally described through staging. The most prevalent scheme is the TNM Staging System, which describes the extent to which cancer is present in the primary tumor (T), regional lymph nodes (N), and metastatic sites (M). This method was developed by the American Joint Committee on Cancer (AJCC) in order to standardize classification. In the case of prostate cancer, the value for T is determined both clinically and pathologically, with T0 indicating an undetectable primary tumor, while T4 indicates disease which has invaded tissues beyond the sex accessory tissues. The value for N is designated 1 or 0 to indicate the presence or absence of metastases in regional lymph nodes; M is similarly defined, with additional distinctions for a

value of 1 to indicate the metastatic site as distant lymph nodes (1a), bone (1b), or another tissue (1c) [16].

While staging provides a valuable framework through which to understand prostate cancer, histological examination of cancerous tissue remains the gold standard of disease evaluation. For primary disease, this involves determination of the Gleason score, a grading system based on glandular morphology observed over two distinct biopsy regions which reflects the overall status of the cancerous tissue. First, a tissue sample is surveyed in order to identify the two most common tumor patterns. Each of these patterns is then examined closely and given a grade ranging from 1-5, with one indicating well-differentiated glandular structure and five indicating anaplastic morphology with no clear glands. These values are summed, giving a final grade of 2-10. Upon analysis of patient outcomes, a strong positive correlation was found between Gleason grade and clinical stage of the patient, with the highest scores predicting poor prognosis and decreased survival [17]. Further study has established the predictive value of Gleason grading, with patients with scores six and under having an excellent prognosis, while those with grades 7-10 having more aggressive tumors which are expected to metastasize. By combining both Gleason grade and TNM stage, an accurate prediction can be made regarding prognosis and likely patient outcomes [5].

In addition to the aforementioned approaches, the occurrence and progression of prostate carcinoma is often evaluated through the proxy of blood serum prostate-specific antigen (PSA) levels. PSA expression is highly specific to prostate epithelial cells, where it is regulated via the androgen receptor; cancer leads to increased levels which can be detected in the serum [8]. Unfortunately, because expression is shared by both benign and malignant prostate cells, PSA also rises in the case of BPH or inflammation of the prostate [3]. Thus, although this method is controversial due to the potential hazard of over-diagnosis and overtreatment, its use remains widespread for both screening and monitoring purposes. Although advice varies, the current recommendation from the American Urological Association prescribes PSA screening among the general population only for men aged 55-69 who choose to test after "shared decision-making" with their healthcare provider, and then with no more than biennial frequency [9], while the U.S. Preventative Services Task Force universally advises against using serum PSA to screen for prostate cancer [18]. Men with a strong family history or other substantial risk factors, however, are more likely to benefit from regular PSA testing, particularly when combined with other screening methodologies such as DRE.

For men who have already been diagnosed with carcinoma of the prostate, the change in PSA levels over time, known as PSA velocity, can provide valuable

insight into the status of prostate-derived cells, especially for monitoring of post-treatment individuals. A marked increase in PSA velocity in such patients is termed biochemical recurrence and often indicates the reemergence of malignant disease before it can be recognized through other means. In this regard regular assessment of serum PSA levels is a crucial component of patient care, but it cannot alone supply any data regarding the presence or absence of metastasis [8].

As with other cancers, prostate adenocarcinoma shows a tendency to spread to a predictable set of tissues within the body. PCa preferentially metastasizes to the bone, and at the time of death 90% of patients with known prostate cancer exhibit bone metastases [10]. In addition to a dismal five-year survival rate [19], patients diagnosed with bone metastasis commonly experience serious detriments to quality of life due to pain, pathological fractures, and spinal cord compression. Furthermore, while recently developed therapies such as bisphosphonates and endothelin A receptor antagonists have provided welcome palliation of skeletal symptoms and modest improvements in patient survival, the current standard of care continues to rely on systemic cytotoxic interventions and curative treatments for bone metastasis remain out of reach [20]. The aim of the work described in this dissertation is to address the urgent need for therapeutics which specifically inhibit the development and progression of bone metastases from PCa.

The skeletal tropism of disseminated tumor cells (DTCs) from PCa has long been known, with the predominant bones involved being the vertebrae, pelvis, and ribs [21]. Bone scans of patients with advanced PCa *(Fig. 1)* show the distribution of bone metastatic lesions in the axial and proximal appendicular skeleton, recognized to be a precise overlay of the regions of active hematopoiesis in the adult [22]. That PCa cells spread by the arterial hematogenous route is apparent; the extent to which the pattern of DTC distribution depends on mechanical trapping versus specific molecular affinity between PCa cells and the bone stroma remains unclear [23]. However, it is well established that bone stromal-derived proteins such as TGF-β favor the development of macrometastases [24].

Prostate cancer cells clearly thrive in the environment provided by the bone marrow, and PCa patients diagnosed with skeletal metastases inevitably face worsening symptoms as a result; researchers have long sought to understand the particular biochemical synergy which exists between the bone microenvironment (BME) and invading cancer cells. Much research emphasis has been placed on the "vicious cycle" of PCa bone metastasis, wherein cancer cells disrupt bone homeostasis by recruiting and activating osteoclasts, which through enhanced bone resorption mobilize factors that drive further growth of the metastatic tumor [25]. Unfortunately, clinical use of bisphosphonates to inhibit osteoclast activity

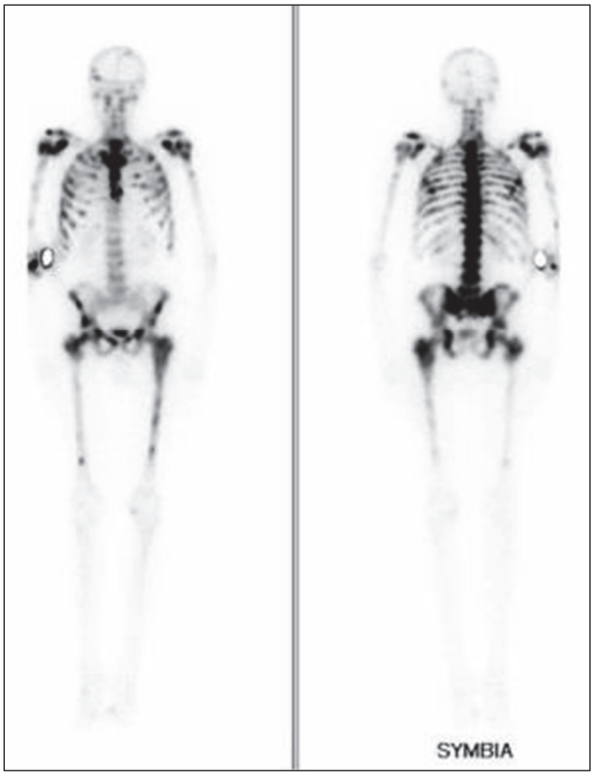

Figure 1: Tc99m radionucleotide bone scan of a 70-year-old patient with advanced meta-static PCa. The dark patches indicate locations of metastatic lesions within the skeleton; this pattern overlaps the distribution of hematopoietically active bone marrow in the adult, suggesting an affinity by PCa cells for active marrow. © Paul M Michaud MD, used with permission.

has not provided the hoped-for gains in survival for patients with bone metastatic PCa [20], calling into question the validity of the "vicious cycle" hypothesis.

While updated models are often proposed, true molecular understanding of the metastatic process has remained frustratingly elusive. In the present situation, therapies that are able to provide meaningful improvements in survival and quality of life among patients who already show signs disseminated disease must be the highest priority, since the needs of these patients cannot be addressed by the current standard of care. The data presented in this thesis offers a novel framework for understanding the development of bone metastasis from prostate adenocarcinoma, and provides a foundation for advanced treatment strategies which would specifically target crucial metastatic processes.

Chapter 2: Experimental Methods & Approach

Introduction

Prostate cancer is the fourth most prevalent malignancy across the global population and the second most prevalent cancer among men, according to a 2012 dataset; it is the fifth leading cause of cancer death among men worldwide [26]. This disparity in prevalence and mortality ranking suggests correctly that PCa is on average less deadly than other cancers, such as those of the stomach or lungs. However, a great deal of the difficulty in appropriately treating PCa is due to the unpredictable progression of the disease. Aggressive treatment, including radio- and chemotherapy, is often pursued when patients are found to have predictors of metastasis such as high Gleason score or rapid increase in PSA, but these markers have proven unreliable in predicting long-term outcomes, especially once changes in androgen signaling develop; more precise biomarkers of PCa progression so far remain obscure.

While cytotoxic therapies may be effective against even locally invasive disease, a proportion of patients receiving this treatment will have undetected bone metastases. Other patients do not receive a diagnosis of prostate cancer until

the disease has already spread. In either case, the options for these individuals unfortunately shift to disease management and palliation, since bone metastatic PCa remains incurable using current methods [20, 27]. Our inability to accurately stratify individuals with indolent disease versus those with more high-risk forms represents a serious weakness in the modern approach to care. We thus adopt as our focus the discovery of novel treatments which limit or prevent the development of bone metastasis.

Much current research into prostate adenocarcinoma follows the structure typical to the cancer field: *in vitro* studies examining the behavior of cancer cells either alone or in combination with other cell types, use of some form of animal model, and analysis of human disease samples or datasets. Human patient samples must necessarily be the gold standard of cancer research, but for pre-clinical studies this data is by definition observational, and causative conclusions cannot be made from it. Cell lines derived from human patients are probably the most widely-used tool in cancer research, but these cells will be assessed largely in an environment very different from that whence they came, potentially altering their behavior and misleading investigators. While the process of carcinogenesis itself may be recapitulated using sophisticated tissue culture techniques, it is very challenging to recreate the complexity of the circumstances surrounding metastasis *in vitro*.

Pre-clinical animal models offer many more options, each with its own strengths and weaknesses. Traditionally, mouse studies generally fall into one of two categories: genetically engineered animals which, due to one or more mutations, spontaneously produce tumors in the relevant tissue, or xenograft transplantation of tumor cells or tissue into animals which generally must be immunocompromised in order not to reject the grafted tissue. Transgenic animals that spontaneously form tumors have the benefit of being otherwise healthy animals which play host to the entire course of oncogenesis, providing a more complete view to researchers. However, these models often rely on already well-known oncogenes to propel tumor formation, thereby neglecting the possibility of novel drivers more relevant to human disease. Furthermore, the cancer progression in these animals may not follow the same pattern seen in patients, raising questions about the validity of the model.

For xenograft-based studies, the opportunity to graft either cultured or primary human cancer cells into the animal is a huge strength, but the necessity of immunocompromised mice eliminates cell-mediated immunity from the environment with which the cancer cells contend, ignoring the possible significant role of the immune system. Additionally, xenografts may be performed in a variety of different ways, with each variation potentially affecting the quality of the resulting data.

In the field of prostate cancer, the transgenic adenocarcinoma mouse prostate (TRAMP) model is one of the earliest. This line utilizes a truncated version of the prostate-specific rat probasin (PB) promotor to drive expression within the prostate of the oncogenic SV40 early region, which contains both the large-T antigen (Tag) and small-t antigen [28]. These animals develop prostatic hyperplasia as early as 10 weeks of age, and progress to fully developed adenocarcinoma by four months [29]. By six months of age, 100% of animals show lymph node metastasis, while 67% have metastasis to the lung; the cells which make up these tumors tend to have decreased expression of the androgen receptor. Bone metastases have been reported in some TRAMP animals, but this varies by genetic background and a number of other factors, making this an unreliable model for the study of skeletal metastasis. Furthermore, pulmonary metastasis is uncommon in human PCa patients, and cancer cells recovered from castrated TRAMP animals were universally positive for neuroendocrine markers, suggesting that this system more closely models the rare neuroendocrine prostate cancer rather than the far more common adenocarcinoma. A similar model, dubbed LADY, uses Tag alone and results in slower development of malignancy, but still predominantly results in visceral metastases with neuroendocrine features [28].

Other transgenic lines include those with targeted deletion of the tumor suppressor PTEN or overexpression of the Myc oncogene within the mouse prostate. These models both provide a reliable manifestation of prostatic intraepithelial neoplasia (PIN), often progressing to hyperplasia and even fully-fledged adenocarcinoma, but they exhibit a fair amount of inconsistency in tumor phenotype and have not been shown to reliably progress beyond lymphatic invasion, making them a poor choice for the study of metastasis [28, 29].

The most straightforward and frequently seen form of xenograft in cancer research is the ectopic subcutaneous injection of cultured cancer cells, most often on the animal's flank [30]. Because relatively large volumes can be tolerated in this anatomical region, researches may inoculate tens of millions of cells with no ill effects; they may also include artificial matrix such as Matrigel in order to aid the development of the xenografted tumor. Using tumorigenic cells, this method consistently produces tumors which can readily be observed and later isolated for analysis. However, the microenvironment of this region, sandwiched between skin and muscle on a mouse's back, is unlikely to recreate the molecular milieu to be found in the prostate; while it may be preferable to tissue culture, flank injection essentially tasks the mouse with providing biological support to the cells, and does not generally enable the cancer cells to spread to distant sites, making it a nonviable choice for the study of metastasis.

An improvement on the ectopic approach is the orthotopic xenograft, wherein the cells are introduced directly into the organ analogous to their tissue of origin. While this technique is valuable when examining earlier stages such as progression and invasion, it does not necessarily allow for metastatic progression, and can be technically challenging when studying deep internal organs such as the prostate, making it less relevant to the study at hand.

In order to truly study metastasis, xenografted cancer cells must have access to the bloodstream. One option which permits blood-born spread of inoculated cells is injection via the lateral tail vein of a mouse. Animals treated in this way form no primary tumor, with the cancer cells seeding and proliferating in whatever tissue they are able. However, in prostate cancer these models most often produce metastatic lesions in the lung and liver, likely as a result of mechanical filtering of the cancer cells from the venous blood restricting the innate cellular tropism [31]. As was seen in some of the transgenic models, this pattern of metastasis is not representative of what is seen in human disease, and therefore limits the practicality of this model.

Our model system relies on intracardiac injection of fluorescently-labeled human PCa cell lines into immunocompromised mice; intra-arterial inoculation enables us to introduce circulating tumor cells (CTCs) of known quantity and characteristics, and permits unbiased homing of the cells to any tissue in the body

without the complication of premature mechanical trapping in the pulmonary vasculature [31]. Using this method, our lab has shown reproducible patterns of metastasis consistent with what is observed clinically in both breast [32] and prostate [33] cancer metastasis, supporting the claim that this method does not restrict or alter cancer cell tropism.

In our method, fluorescently-labeled polystyrene beads are co-injected with the PCa cells and will lodge in the kidney parenchyma if introduced to the arterial circulation, allowing for independent verification of proper inoculation in each animal; luciferase-labeling of PCa cells provides still further confirmation of whole-body distribution of CTCs *(Fig. 2)*, and permits longitudinal monitoring and quantification of lesion development throughout an experiment.

Hematopoiesis in rodents occurs in the long bones throughout the animal's life [34], making the knee joint a frequent site for the development of metastatic lesions which recapitulate the course of human disease. Complete serial sectioning of fixed frozen tissue allows us to enumerate tumor foci across both knee joints of each animal, and fluorescent microscopy using the Nuance multispectral imaging system enables detection and measurement of lesions ranging from macro-metastases to individual DTCs *(Fig. 3)*. Finally, laser capture micro-dissection (LCM) makes possible the precise isolation of regions of interest from these same tissue sections in quantities sufficient for molecular analysis,

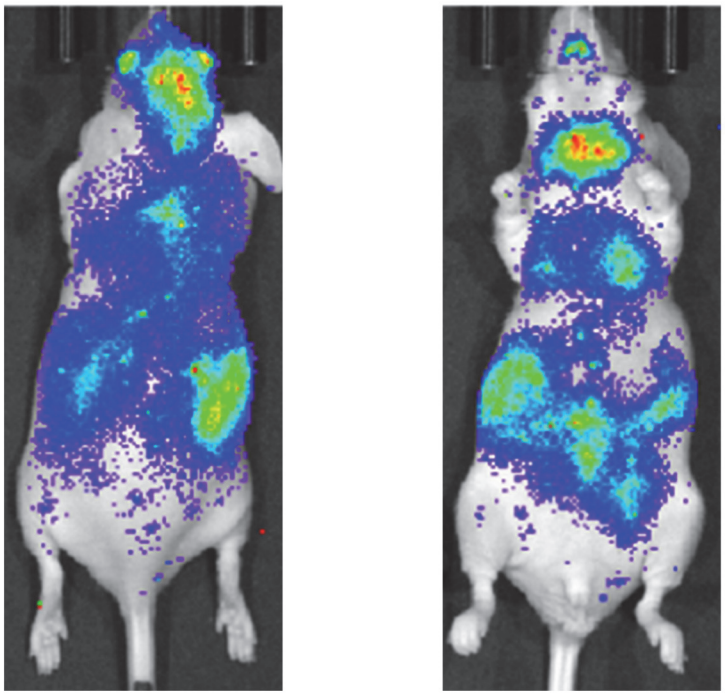

Figure 2: *In vivo* bio-luminescent imaging showing the distribution of CTCs one hour after intra-cardiac inoculation of 5×10^5 luciferase-expressing PCa cells.

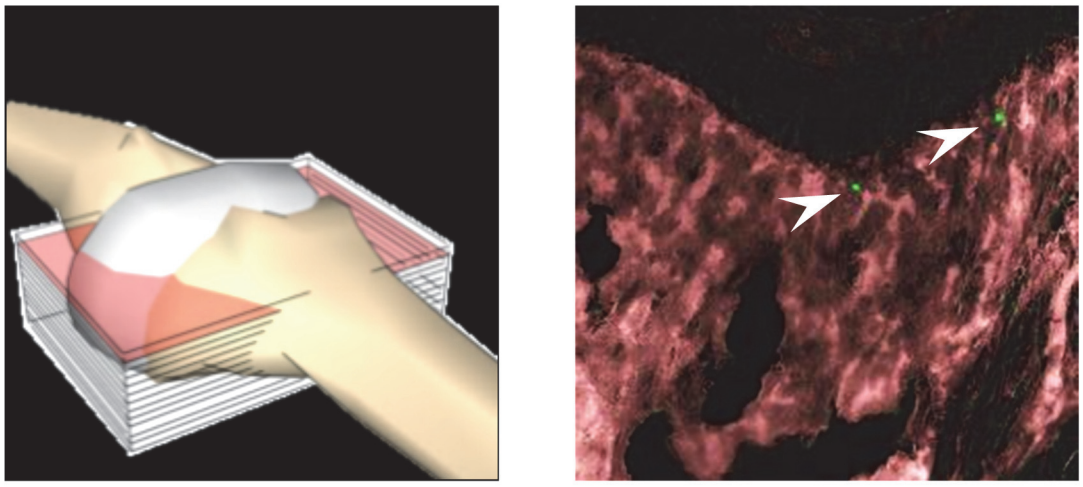

Figure 3: *(left)* Schematic showing comprehensive serial sectioning of the fixed and frozen mouse knee joint. *(right)* Fluorescent micrograph showing GFP-labeled DTCs (arrows) in the knee five minutes after intracardiac inoculation (10X).

including expression profiling studies such as Nanostring. Together, these methods provide a direct, innovative, and powerful translational methodology for analyzing *in vivo* metastatic phenotypes of prostate cancer cells, allowing for the incorporation of various genetic and pharmacological interventions: all this provides a robust basis for future clinical studies.

Materials and Methods

Cell lines and culture

DU-145, 22Rv1, LNCaP, and VCaP human prostate cancer cell lines were purchased from ATCC; the PC3-ML cell line was derived from the parental PC-3 cell line as previously described [35]. All cell lines were authenticated by short tandem repeat profiling by IDEXX Radil (Columbia, MO) and/or DDC Medical (Fairfield, OH). Cells were cultured in Dulbecco's Modified Eagle Medium (Gibco, Waltham, MA, USA) (DU-145, VCaP, and PC3-ML) or RPMI-1460 (Gibco) (22Rv1 and LNCaP) containing 10% fetal bovine serum (HyClone Laboratories, Logan, Utah, USA) and 0.1% gentamicin (Invitrogen, Waltham, MA, USA). Bone marrow-derived Human Mesenchymal Stem cells (Lonza, Allendale, NJ) were used between passage 5 and 8 and cultured in α-MEM (Gibco) supplemented with 10% FBS, 1 ng/ml bFGF (R&D Systems, Minneapolis, MN), and 0.1% gentamicin. Each cell line was cultured at 37°C and 5% CO2 and discarded 10 passages following thawing.

Conditioned media were obtained according to [36]. In brief, 7.5 x 10^5 PC3-ML cells were plated in 15 ml of DMEM supplemented with 10% fetal bovine serum and 0.1% gentamicin and cultured for five days. The medium from each dish was then collected and centrifuged at 2000 rpm for 10 minutes, then used fresh as described.

Viral Vectors for Stable Gene Expression

Stable expression of the fluorescent markers eGFP and mCherry, the luciferase enzymes Red Firefly Luciferase and Luc2, and the cytokine IL-1β were achieved through lentiviral transduction with the following constructs: pLenti CMV GFP Blast (659-1), pLenti CMV Blast empty (w263-1), pLenti CMV Puro DEST (w118-1), and pENTR1A no ccDB (w48-1) were gifts from Eric Campeau (Addgene plasmids # 17445, 17486, 17452, and 17398). pLenti CMV mCherry Blast was produced by subcloning the mCherry gene from pmCherry-N1 (Clontech, Mountain View, CA, USA) into the BamHI and XbaI sites of pLenti CMV Blast empty. pLenti CMV Red Luc Puro and pLenti CMV Luc2 Puro were produced by first subcloning the Red Firefly Luciferase gene from pMCS-Red Firefly Luc (Thermo Fisher Scientific, Waltham, MA, USA) or the Luc2 gene from pGL4.51[luc2/CMV/Neo] (Clontech) into the BamHI and XhoI sites of pENTR1A no ccDB; pLenti CMV IL-1β Puro was produced by initially shuttling human IL-1β cDNA (NM_000576) into the SalI and BamHI sites of pENTRA1A no ccdB. Each

of these inserts was then transferred via Gateway LR Clonase II (Invitrogen) into pLenti CMV Puro DEST. Following lentiviral transduction, cells were selected with puromycin or blasticidin for one week at the following concentrations, respectively: PC3-ML: 600 ng/mL, 5 μg/mL. 22Rv1: 1 μg/mL, 6 μg/mL. DU-145: 500 ng/mL, 10 μg/mL. LNCaP: 2 μg/mL, 7 μg/mL. VCaP: 2 μg/mL, 7 μg/mL.

SDS-PAGE

Cells were washed with ice-cold balanced salt solution and scraped in lysis buffer (50 mM Tris, 150 mM NaCl, 0.5% sodium deoxycholate, 0.1% sodium dodecyl sulfate (SDS), 10 mM Na4P2O7, 5 mM ethylenediaminetetra-acetic acid [EDTA], 1% Triton X-100, 1 mM dithiothreitol, with protease (Calbiochem, cat#539134) and phosphatase (Calbiochem, cat#524625) inhibitor cocktails). Equal amounts of proteins as determined by the bicinchoninic acid assay from Thermo Scientific (Rockford, IL) were loaded in each lane, separated by sodium dodecyl sulfate–polyacrylamide gel electrophoresis (SDS-PAGE), and transferred to polyvinylidene fluoride membranes for immunoblotting.

Western Blotting

Primary antibodies were diluted in TBST and membranes incubated overnight at 4°C. HRP-conjugated secondary antibodies (Goat anti-Mouse IgG #32430 and Goat anti-Rabbit IgG #32460, Pierce) were used at 3.33 ng/mL. Chemiluminescent signals were obtained using SuperSignal West Femto substrate

(Pierce) and detected with the Fluorochem 8900 imaging system and related software (ProteinSimple, Santa Clara, CA, USA). Primary antibodies used for Western Blotting were those targeting S100A4 (ab27957, Abcam, Cambridge, UK); IL-1β (SC-7884, Santa Cruz Biotechnology, Dallas, TX, USA); phospho-IκBα Ser32 (#2859), IκBα (#4814), phospho-NF-κB p65 Ser536 (#3033), NF-κB p65 (#8242 all Cell Signaling Technology, Beverly, MA, USA); Actin (A-2066, Sigma-Aldrich) and GAPDH (#5174, Cell Signaling Technology) were employed as loading controls.

Animal models

Male C.B17-SC mice (Taconic, Germantown, NY, USA) were housed in a germ-free barrier. At six to eight weeks of age, mice were anesthetized with the combined administration of ketamine (80 mg/kg) and xylazine (10 mg/kg) administered by intraperitoneal route and then inoculated in the left cardiac ventricle with the indicated quantity of human prostate cancer cells suspended in 100 μL phenol red-free DMDM/F12 (Gibco). Cell inoculation was performed using a 1 mL syringe with a 30-gauge needle. The correct execution of intracardiac inoculation was established by the appearance of pulsating fresh blood in the fitting of the hypodermic needle, which indicated the successful penetration of the ventricular wall. In addition, blue-fluorescent polystyrene beads (10 μm diameter, Invitrogen-Molecular Probes) were co-injected with cancer cells; their detection by

fluorescence microscopy in the kidneys at necropsy confirmed the successful inoculation in the arterial blood circulation.

For experiments involving anakinra treatment, animals received an initial subcutaneous dose of vehicle (PBS) or anakinra (Swedish Orphan Biovitrum AB, Stockholm, Sweden) 24 hours prior to cancer cell inoculation, then additional doses at the time of xenograft and daily thereafter until sacrifice.

All experiments were performed in accordance with NIH guidelines for the humane use of animals. The Drexel University College of Medicine Institutional Animal Care and Use Committee approved all protocols involving the use of animals.

Generation of IL-1R SCID mice

IL-1R SCID mice were generated by crossing C.B17-SC mice with transgenic animals with a knockout of *IL-1R1* (OMIM 147810, a gift from Nancy McNamara, Ph.D., O.D., University of California San Francisco). These animals were then genotyped for the *Prkdc*^{scid} mutation by PCR using the forward primer 5′ GGA AAA GAA TTG GTA TCC AC 3′ and reverse 5′ AGT TAT AAC AGC TGG GTT GGC 3′; the product in each case was then digested with AluI (New England Biolabs, Ipswich, MA, USA), resulting in fragments of 68 and 11 bp in the case of wild-type and 38, 28, and 11 bp in the case of SCID. IL-1R status was determined by mutiplex PCR using the following primers: IL-1R WT Fwd- 5′ CCA CAT ATT

CTC CAT CAT CTC TGC TGG TA 3′, IL-1R WT Rev- 5′ TTT CGA ATC TCA GTT GTC AAG TGT GTC CC 3′, IL-1R KO Fwd- 5′ CTG AAT GAA CTG CAG GAC GA 3′, IL-1R KO Rev- 5′ ATA CTT TCT CGG CAG GAG CA 3′, and resulting in amplification of fragments of 350 base pairs in the presence of the wild-type allele and 172 base pairs in the case of the knockout *(Fig. 4)*. Once animals homozygous for *Prkdc*^{scid} and heterozygous for IL-1R were obtained the colony was maintained through intercross of IL-1R heterozygotes, with six- to eight-week-old male wild-type and knockout littermates being used in the experiments described.

In vivo bioluminescence imaging

Prior to each weekly imaging session, animals were injected IP with 150 mg/kg D-Luciferin - K+ Salt Bioluminescent Substrate (PerkinElmer) and allowed to rest for ten minutes. Mice were then anesthetized using 3% isoflurane and transferred to the chamber of an IVIS Lumina XR (PerkinElmer), where they received 2% isoflurane throughout image acquisition. Fifteen minutes after injection of the substrate, exposures of both dorsal and ventral views were acquired both without an emission filter and with the 515-575 nm band pass filter; at the end of each experiment, radiographs were taken of each animal. Analysis of these data was performed using Living Image software, v4.3.

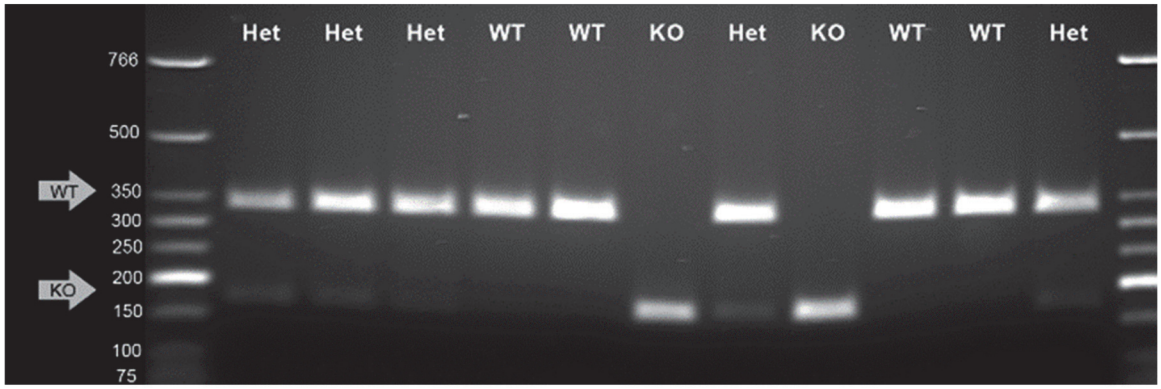

Figure 4: Typical gel image of IL-1R mouse genotyping by polymerase chain reaction; using a multiplex program, DNA fragments of 172 base pairs (knockout) and 350 base pairs (wildtype) were amplified in a single reaction. Samples were then run on a 1.5% agarose-TBE gel, stained with ethidium bromide, and imaged on a UV transilluminator; notations across the top show the indicated genotype for each animal.

Processing of animal tissues.

Bones and soft-tissue organs were collected and fixed in 4% paraformaldehyde solution (Electron Microscopy Sciences, Hatfield, PA) for 24 hours and then transferred into fresh formaldehyde for an additional 24 hours. Soft tissues were then placed either in 30% sucrose for cryoprotection or 1% paraformaldehyde for long-term storage. Bones were decalcified in 20% EDTA (Fisher Scientific, Leicestershire, UK) for 7 days followed by incubation in 30% sucrose. Tissues were maintained at 4°C for all aforementioned steps and frozen in O.C.T. medium (Sakura Finetek, Torrance, CA) by placement in powdered dry ice. Serial sections of 80μm thickness were obtained using a Microm HM550 cryostat. Femur and tibia in each knee joint were cut entirely through, resulting in approximately 30 sections per specimen made available for analysis. All sections spanning the entire bone width were inspected to obtain accurate enumeration of DTCs as well as visualization and size measurement of tumor foci in the inoculated animals.

Fluorescence microscopy and morphometric analysis of animal metastases

Fluorescent images of skeletal metastases were acquired using a Zeiss AX70 microscope (Carl Zeiss, Oberkochen, Germany) connected to a Nuance

Multispectral Imaging System (CRI, Guelph, ON). Digital images were analyzed and processed with the Nuance Software (v. 2.4). Microscope and software calibration for size measurement was performed using a TS-M2 stage micrometer (Oplenic Optronics, Hangzhou City, China). In experiments assessing arrival/colonization of the bone, animals were sacrificed and femora and tibia were imaged and processed using a standardized spectral library, GFP-positive DTCs were enumerated, and total DTC counts in the knee joint each animal were obtained. For quantification of DTCs in the lungs, tissue from the same animals analyzed for bone dissemination was sectioned at 80 μm at intervals across the organ, and images of five random fields obtained as described. After image processing, GFP-positive DTCs were enumerated and summed for each animal. Data from both tumor measurements and DTC counts were subjected to statistical analysis between groups using an unpaired, two-tailed Student's t-test.

Immunofluorescence

For immunofluorescence of primary PCa and bone metastases, Formalin-Fixed Paraffin-Embedded (FFPE) sections were obtained from the archives of the Department of Pathology at Drexel University College of Medicine and stained using a FITC-conjugated Pan-Cytokeratin antibody (clone C-11, Sigma Aldrich) and an antibody against the N-20 region of the human Androgen Receptor (Bethyl Laboratories, Montgomery, TX, USA; a gift from Dr. Karen Knudsen, Sidney

Kimmel Cancer Center at Thomas Jefferson University) followed by an anti-rabbit Alexafluor 568 secondary antibody (Invitrogen). These samples were then imaged by conventional fluorescence microscopy using an Axio Scope A1 microscope (Zeiss) paired with the Nuance Multispectral Imaging System (PerkinElmer, Waltham, MA, USA).

For staining of hMSCs, cells were seeded onto glass coverslips and treated, then fixed in 4% paraformaldehyde for 15 minutes at room temperature and stained with Anti-Actin, α-Smooth Muscle - Cy3™ (clone 1A4, Sigma-Aldrich). Stained samples were then mounted with DAPI-contained medium (Vector Laboratories, Burlingame, CA, USA) and imaged via confocal microscopy using an LSM 5 Exciter – Axio Imager Z1m (Carl Zeiss, Oberkochen, Germany).

Immunohistochemistry and analysis of human bone metastases

De-identified FFPE biopsy specimens of bone metastatic lesions from two different cohorts of ADT-treated advanced prostate cancer patients were obtained from the archives of the Departments of Pathology at Drexel University College of Medicine (5 patients) and at Thomas Jefferson University (4 patients), and stained using the aforementioned antibody against the N-20 region of the human Androgen Receptor, or against Prostein (Clone 10E3, Dako, Glostrup, Denmark). These biopsy specimens were used to determine the relative percentage of AR+ and AR− PCa cells across 43 distinct regions of interest. Two certified pathologists

(F.U.G and Y.G) selected the tumor areas to be inspected for AR expression by examining paired serial sections stained with Hematoxylin/Eosin. Assessment of AR staining intensity was performed using the Aperio system and ImageScope software (Leica Biosystems, Nussloch, Germany). Immunohistochemistry signals were digitized and analyzed by scoring staining intensity as high (3+), medium (2+) and low (1+), with absence of nuclear AR staining scored as (0).

Laser Capture Microdissection

Mouse tissues for LCM were prepared and frozen in OCT compound as described, then sectioned at 40-μm thickness. Tissue slides were washed with ice-cold RNase-free water for 2 minutes to remove OCT compound, then immediately dehydrated using an ethanol gradient in order to maintain RNA integrity. Human FFPE sections subsequent to those used for IHC were deparaffinized in ice-cold xylene substitute for 15 minutes and dehydrated in ethanol for 30 seconds. LCM was performed using a PALM MicroBeam system (Zeiss). Microdissected tissues were catapulted into Zeiss AdhesiveCap 200 tubes and stored at −80 °C until RNA extraction.

qRT-PCR

Microdissected tissue samples were slowly thawed at room temperature, followed by RNA extraction using the RNeasy FFPE Kit (Qiagen, Venlo, Netherlands) according to the "LCM Protocols - RNA Handling" manual available

from Zeiss. Human RNA samples were amplified using the Ovation Pico WTA system V2 (NuGEN Technologies, San Carlos, CA, USA). Extracted mouse RNA samples and amplified human cDNA samples were stored at −80 °C until qRT-PCR was performed using an Applied Biosystems 7900HT Fast Real-Time PCR System. Gene-specific primer-probe sets were purchased from Applied Biosystems/Life Technologies and are listed in *Table 1*.

Nanostring Profiling

For Nanostring transcriptome analysis we used 100ng of total RNA (20ng/μl) on the nCounter Pan Cancer immune profiling for mouse, which includes 750 genes with established relevance in immune response plus 40 housekeeping genes used for normalization and selected with a geNorm algorithm. The nSolver (v.2.5) user interface was used to operate the nCounter Advanced analysis module, which employs the R statistical software.

Table 1: Primer-probe sets used for qRT-PCR analysis.

Species	Protein	Gene Symbol	TaqMan Assay ID
Human	Prostein	*SLC45A3*	Hs00263832
Human	Androgen Receptor	*AR*	Hs04272737
Human	Interleukin-1β	*IL1B*	Hs01555410_m1
Human	PDGFRα	*PDGFRA*	Hs00998028_m1
Human	GAPDH	*GAPDH*	Hs99999905_m1
Human	Synaptophysin	*SYP*	Hs00300531_m1
Human	Chromogranin A	*CHGA*	Hs00900370_m1
Mouse	GAPDH	*Gapdh*	Mm99999915_g1
Mouse	S100A4	*s100a4*	Mm00803371_m1
Mouse	COX-2	*Ptgs2*	Mm00478374_m1

Chapter 3: Previous Findings

In this section, we will review the previous work produced by the Fatatis laboratory

Identification of novel mediators of bone metastasis

Work in our laboratory has focused on the use of a variety of human-derived prostate cancer cells. Chief among these is the highly bone-metastatic PC3-ML line, which dependably forms bone metastases in over 90% of animals inoculated via the left cardiac ventricle. These cells were derived from the parental PC3 cell line, which was initially obtained from a bone lesion of a patient with advanced PCa, via serial xenograft and isolation of the bone-metastatic population [37]. Their counterpart line, PC3-N, were selected from PC3 cells which failed to invade in repeated Boyden chamber assays; these cells arrive to the bone as efficiently as PC3-ML cells in our animal model, but are incapable of sustaining metastatic development [35, 38]. One notable difference between PC3-ML and PC3-N cells is that the latter do not express the α-isoform of the platelet-derived growth factor receptor (PDGFRα), while the former expresses large quantities [39]. Indeed, exogenous expression of PDGFRα in PC3-N cells imbues them with a metastatic potential equal to that of PC3-ML cells [33, 38].

Additionally, our lab frequently utilizes the DU-145 line, which was derived from a brain metastasis in a patient with stage 4 disease [40]. This cell line is notable for homing to the bone marrow in equal numbers to the PC3 cell lines, but being unable to form tumors or persist beyond 72 hours post-injection. Like PC3-N, DU-145 cells do not express PDGFRα; however, exogenous expression in DU-145s does not increase the metastatic capabilities [39].

In order to identify novel mediators of PCa bone metastasis, we undertook comparative microarray analysis of the cell lines described above. Using a two-fold cutoff, we first compared expression levels in PC3-N and PC3-ML cells, and identified 16 genes as being differentially expressed between the two. We then compared PC3-N cells with PC3-N PDGFRα, resulting in 7 genes found to be upregulated in both PC3-N PDGFRα and PC3-ML relative to PC3-N.

Since PDGFRα expression in DU-145 cells does not alter their metastatic behavior, we included these cells in our analysis in order to eliminate any false positive genes which may become upregulated in response to PDGFRα expression but do not contribute to the metastatic phenotype; of the 5 genes upregulated in DU-145 PDGFRα cells, none overlapped with the previous list.

Finally, in an effort to account for genetic variability among cell populations, clonal progenies derived from individual PC3-ML cells were developed and introduced into our mouse model. Of these, clone 1 and clone 3

were found to be highly bone-metastatic; when included in the microarray analysis, our cohort of genes upregulated in bone metastatic cell lines was winnowed down to three: the inflammatory cytokine IL-1β, the chemokine CXCL6, and the leukocyte protease inhibitor elafin [41].

Validation of the identified genes was first performed on the mRNA level and then by proteomic analysis. The results were further corroborated via the Oncomine data repository, which showed IL-1β, CXCL6, and elafin all to be significantly upregulated in primary prostate cancer as compared with normal prostate tissue. Further meta-analysis of Oncomine datasets revealed that high expression of both IL-1β and CXCL6 significantly correlated with Gleason scores of seven or above. With this data in hand, we obtained a tissue microarray bearing 227 cases of prostate adenocarcinoma and stained for IL-1β. When assessed for IL-1β stain intensity relative to Gleason score, we again observed that the high levels of IL-1β correlate with the highest Gleason scores, validating the Oncomine findings. Given that, as previously mentioned, high Gleason score indicated primary prostate tumors with a greater propensity to metastasize, these data indicate that IL-1β may play the pro-metastatic role suggested by our microarray analysis [41].

Interleukin-1β as a driver of prostate cancer progression

Interleukin-1 (IL-1) is an archetypal pro-inflammatory cytokine, first recognized in the 1940s for its potency as a pyrogen. A considerable variety of rapidly-induced immune responses was soon attributed to the activity of this protein, which was finally identified by molecular means in the mid-1980s [42]. Early researchers were struck by the speed and breadth of biological responses to IL-1 even at femtomolar concentrations; contrasting with the understanding of homeostatic regulation at the time, these features indicated the singular characteristics of this powerful immune mediator [43].

The IL-1 family primarily consists of two agonists, α and β, and one antagonist, IL-1ra. Each of these can serve as a ligand for two membrane-integral toll-like receptors, IL-1RI and IL-1RII. IL-1RI transduces signals via such pathways as NF-κB, p38, and MAP kinase to transcriptionally regulate gene expression, while IL-1RII has no intracellular domain and thereby serves as a decoy receptor, effectively neutralizing any ligand it binds. None of the IL-1 family ligands are known to have an intracellular function, and thus can only exert influence by binding in an autocrine, paracrine, or endocrine manner to a membrane receptor [44].

Interleukin-1 family members are unique among cytokines in including an endogenous full antagonist which is highly effective in counteracting the actions

of the agonists. Indeed, the first investigators to name and characterize IL-1ra were surprised to find it produced by the same cells which secrete IL-1α and β, and binding to IL-1 receptors with comparable affinity, in a system which is highly conserved across evolution. Furthermore, IL-1ra is a remarkably clean antagonist: even at concentrations up to 10 μg/mL, no receptor activation by recombinant IL-1ra was observed [45]. The potential importance of this novel endogenous antagonist in regulating immune response was immediately clear, and multiple studies were published within a year of the first which established, both in vitro and in vivo, the ability of recombinant IL-1ra to directly counter the effects of IL-1α and IL-1β [46, 47]. The therapeutic promise of recombinant human IL-1ra was apparent, and the invention swiftly patented [48, 49] and rebranded as "anakinra" [50]. The US Food and Drug Administration approved anakinra under the brand name Kinaret for the treatment of adult patients with rheumatoid arthritis in November 2001 [51].

IL-1, and IL-1β in particular, have previously been associated with tumor-promoting effects in a variety of malignancies. In a 2003 study, Voronov et al. [52] describe impaired tumorigenesis by both B16 mouse melanoma and DA/3 mouse mammary adenocarcinoma cells injected into the foot pad of IL-1β-null mice, indicating that host-derived IL-1β is advantageous for tumor progression. Furthermore, these same authors identified IL-1β specifically as critical for

angiogenesis in subcutaneous B16 xenografts, suggesting that this cytokine also contributes to metastatic progression. Reviewing the literature in 2006, Lewis et al. [53] observe that the presence of IL-1 in the tumor microenvironment, be it host/stroma- or tumor-derived, enhances the virulence of cancer cells, and that patients whose tumors express high levels of IL-1β face a worse prognosis that those who do not. They further note that IL-1 has been found to be upregulated in human carcinomas of the lung, colon, breast, skin, and head and neck, and propose that IL-1 signaling contributes to a pro-metastatic phenotype by inducing the expression of matrix metalloproteinases (MMPs) and vascular endothelial growth factor (VEGF) among surrounding cells. Ultimately, however, the anticipated function of IL-1β in metastasis relies predominantly on such circumstantial evidence [54-56].

IL-1β promotes skeletal colonization and progression by prostate cancer cells

In light of the strong evidence that IL-1β drives metastatic progression, we employed an IL-1β-targeting short-hairpin RNA (shRNA) to deplete expression and secretion levels in PC3-ML cells to those observed within the PC3-N line [41]. The resultant PC3-ML(sh-IL-1β) cells were delivered into the arterial circulation of mice which were euthanized four weeks later. Inspection of femora and tibiae of these individuals showed that while PC3-ML and PC3-ML(sh-IL-1β) cells produced bone metastases in a comparable number of animals, the lesions

generated by the IL-1β-knockdown PC3-ML cells were 70% smaller than those produced by PC3-ML cells expressing endogenous levels of IL-1β.

To further define the role of IL-1β in skeletal metastasis, our laboratory conducted complementary experiments in which this cytokine was exogenously expressed in prostate cancer cells with a demonstrated inability to generate macroscopic bone lesions in our animal model. DU-145 cells, which are widely reported to lack bone-tropism in mouse models [57] and do not persist in the bone marrow beyond three days *in vivo* [38], do not express IL-1β. Hitherto these cells have never been induced to form skeletal metastases in our hands. However, upon induction of stable IL-1β expression via retroviral vector, DU-145 cells generated *de novo* macroscopic bone lesions in 40% of mice examined four weeks post-inoculation. Furthermore, metastases detected four weeks post-inoculation demonstrated significantly larger tumor area relative to those examined after two weeks, clearly indicating that IL-1β promotes both survival and proliferation of metastatic cells in the skeleton [41].

When considered as a whole, these findings depict a process through which malignant prostate cells utilize the language of immune mediators in order to create favorable circumstances for their own growth and proliferation. The remainder of the work presented here seeks to expand upon this hypothesis in hopes of revealing an Achilles' heel of prostate cancer skeletal metastasis.

Chapter 4: Interleukin-1β in the bone microenvironment

Introduction: Interleukin-1 receptor antagonist as a pharmaceutical

As mentioned in the previous chapter, anakinra is the generic name of recombinant human IL-1ra for pharmaceutical use. Anakinra received FDA approval in 2001 primarily on the basis of a 24-week trial [58] in which participants with chronic rheumatoid arthritis (RA) were divided into four groups and received daily subcutaneous injections of placebo or anakinra at 30, 75, or 150 mg daily. The study revealed a modest but significant percentage of patients achieving the primary outcome of 20% improvement in RA symptoms (ACR20) compared to placebo, regardless of dose. Significant improvement in radiographic assessment in terms of joint erosion as measured by Larsen score and inflammation as measured by erythrocyte sedimentation rate were also found across all anakinra doses, while inflammation as assessed by C-reactive protein levels improved only in the 30 mg/day group. Perhaps most importantly, anakinra was found to have an excellent safety profile, with no difference in withdrawal rates across groups and no difference in adverse events including hospitalization, infection, or malignancy. The only statistically significant adverse event was a

cutaneous reaction at the injection site, which occurred exclusively with the 75 and 150 mg/day dosing regimens.

Ultimately anakinra, under the brand name Kinaret, was distributed by prescription in the format of pre-loaded single-use glass syringes each containing a daily dose of 100 mg, indicated as a second-line agent for RA patients over the age of 18 who has previously failed at least one other disease-modifying anti-rheumatic drug. Although there was initially some concern about a potential increase in infection rates among anakinra-treated patients in a fourth clinical trial which was completed after initial approval, this concern was not borne out in the meta-analysis of five controlled trials conducted by the Cochrane Collaboration [59]. The Cochrane report ultimately concluded that 38% if patients would achieve ACR20 after six months of therapy, compared to 23% of patients receiving placebo over the same time period, with no serious concerns regarding adverse events apart from injection site reactions. A subsequent study followed patients who received daily doses up to 76 weeks of therapy, and revealed no additional adverse outcomes and an incremental improvement in ACR20 at 48 compared to 24 weeks [60]. Thus, despite quite modest improvements in metrics of RA symptoms, it is a remarkably well-tolerated drug even with sustained daily use over the course of almost 18 months. This conclusion further supports the practicality of anakinra as a long-term therapeutic for use among cancer patients.

Anakinra: Preventative treatment

Given our previous findings regarding the importance of IL-1β expression to the bone metastatic behavior of human prostate cancer cells [41], we sought to determine whether this cytokine exerts a functional role in promoting metastasis through experimental interference with its signaling. To strictly address the clinical scenario of advanced prostate cancer in a pre-clinical setting, we focused on late stages of the metastatic process: bone colonization and progression into macroscopic skeletal lesions. Stably fluorescent PC3-ML cells were inoculated in the left cardiac ventricle of mice pretreated for one day with infusions of either vehicle or the IL-1R antagonist anakinra; these treatments continued daily for two weeks until sacrifice. Animals treated with anakinra showed a significant and dose-dependent reduction in tumor burden *(Fig. 5)* as compared to controls. Notably, the impairment in tumor growth observed in animals treated with 40 mg/kg of anakinra equaled the results we obtained in a previous study by silencing IL-1β expression via RNA interference *(Fig. 6)* [41].

Anakinra: Treatment of established metastases

In a coordinating study, we evaluated a curative approach to prostate cancer bone metastasis using the recombinant IL-1 receptor antagonist anakinra. In this model, male SCID mice were inoculated with fluorescently- and bioluminescently-labeled PC3-ML cells, which were allowed to establish

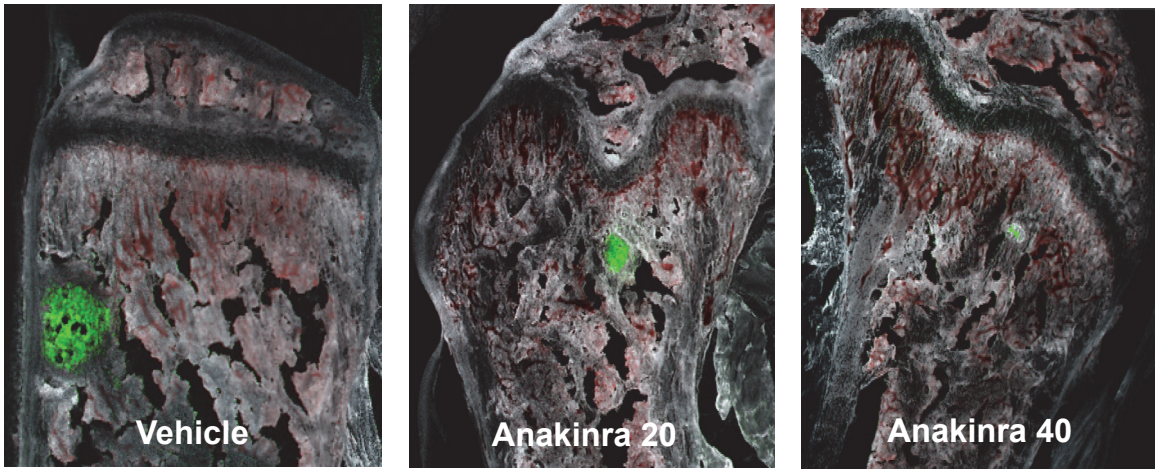

Figure 5: Dose-dependent reduction in tumor burden in response to anakinra treatment. Male SCID mice were pre-treated for one day with the indicated compound, then inoculated with 5×10^5 luciferase-labeled PC3-ML cells. Animals received daily subcutaneous dosing until sacrifice two weeks after the cells were introduced. Numbers indicate dose in mg/kg; n=5-10 animals for each group.

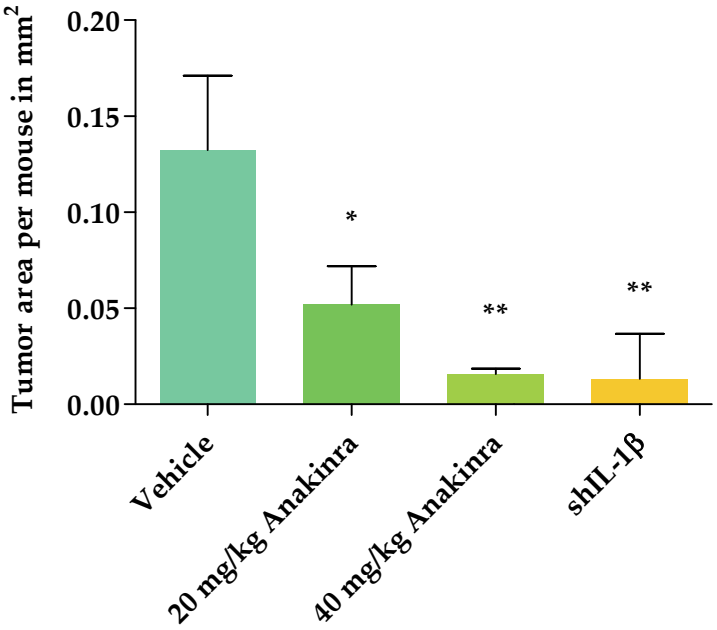

Figure 6: Quantification of tumor burden from the animals in *Fig. 5.* Total tumor burden per mouse was ascertained by measuring the size of each tumor detected in both knee joints of each animal when inspected by multispectral fluorescence microscopy, revealing a dose-dependent reduction in tumor burden in response to anakinra treatment: at the higher dose, comparable to that resulting from IL-1β knockdown in PC3-ML cells; * indicates $p<0.05$; ** indicates $p<0.01$.

themselves for two weeks prior to initiation of treatment with vehicle or 40 mg/kg anakinra. Daily dosing was performed for a further two weeks, at which point the animals were sacrificed. Weekly bioluminescent imaging throughout the course of the experiment, as well as fluorescent microscopy of the resulting tissue samples, evidenced no effect of anakinra treatment relative to vehicle control over this time period *(Fig. 7)*. These results suggest that the critical function of IL-1β signaling in this system is an early event, with alternate schemes providing for the further progression of metastatic disease once prostate cancer cells have established themselves in the bone.

Bone metastasis is inhibited in IL-1R-null animals

Having established both that cancer cell-derived IL-1β drives bone metastasis [41] and that pharmacologic inhibition of IL-1 signaling suppresses metastatic colonization by highly aggressive PCa cells, we next sought to determine the directionality of IL-1 signal transduction in the bone metastatic niche. From a mechanistic standpoint, tumor-derived IL-1β could act in a paracrine fashion on the surrounding bone stroma, which might then reciprocate by providing crucial trophic support for tumor growth. Equally, such IL-1β could act in an autocrine fashion, directly stimulating the cancer cells themselves to take on a pro-metastatic phenotype. To specifically address this issue, we interbred NOD mice null for the Interleukin-1 Receptor (IL-1R, IL1R1) with SCID animals in

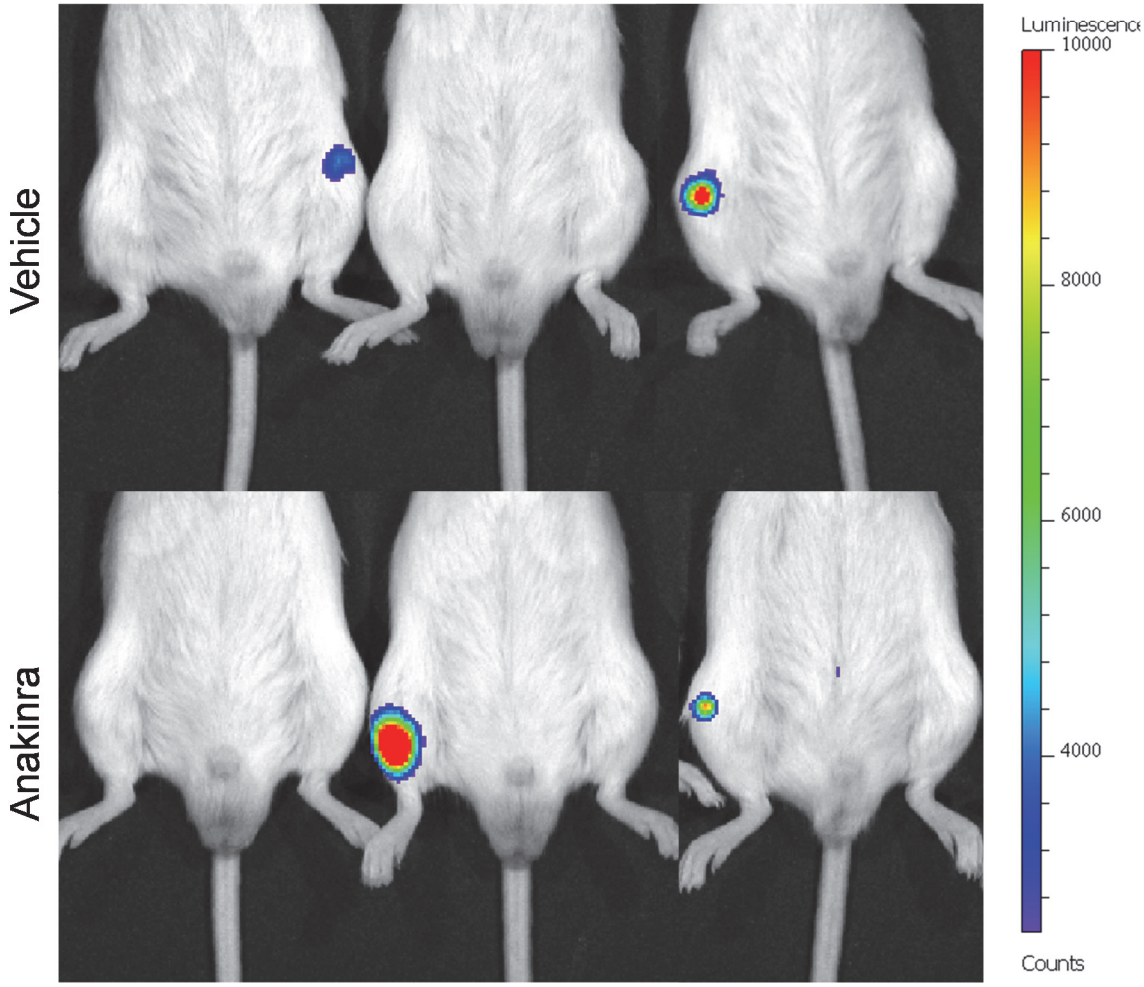

Figure 7: Bioluminescent imaging of SCID mice bearing established PC3-ML tumors: male SCID mice inoculated with 5×10^5 luciferase-labeled PC3-ML cells, and the tumors allowed to develop for two weeks. The animals were then treated for two weeks with vehicle (top) or 40 mg/kg anakinra (bottom), but no difference in tumor progression was noted. n=5 animals per group

order to produce a strain that would be receptive to grafts of human cancer cells under variable conditions of IL-1R expression. We then inoculated IL-1R-null individuals and their wild-type littermates with GFP-labeled PC3-ML cells, sacrificing after two weeks *(Fig. 8)*. In these experiments, IL-1R knockout animals were found to harbor metastases in the knee joint in only 50% of individuals, compared to a 100% metastasis rate in IL-1R wild-type counterparts *(Fig. 9)*. Furthermore, the tumor burden that did exist in IL-1R knock-out mice was on average less than one-tenth that found in the wild-type littermates *(Fig. 10)*. In comparing these data to that obtained in SCID mice inoculated with PC3-ML cells stably expressing shRNA targeting IL-1β, we find a comparable decrease in tumor burden [41]. Taken together, we can deduce that much, if not all, of the pro-metastatic effect of IL-1β is exerted via stromal responsiveness to this cytokine.

Chapter conclusion: IL-1β-mediated bone metastasis requires paracrine signaling between cancer cells and host tissue

Previous work in our lab has demonstrated that osteoclast recruitment to bone metastases occurs only after the attainment of substantial tumor size in a preclinical model, suggesting that the earlier conversion of PCa DTCs to metastatic lesions is mediated through an alternate process [38]. In pursuing this, we found that high expression of IL-1β in PCa cells dictates metastatic behavior in our

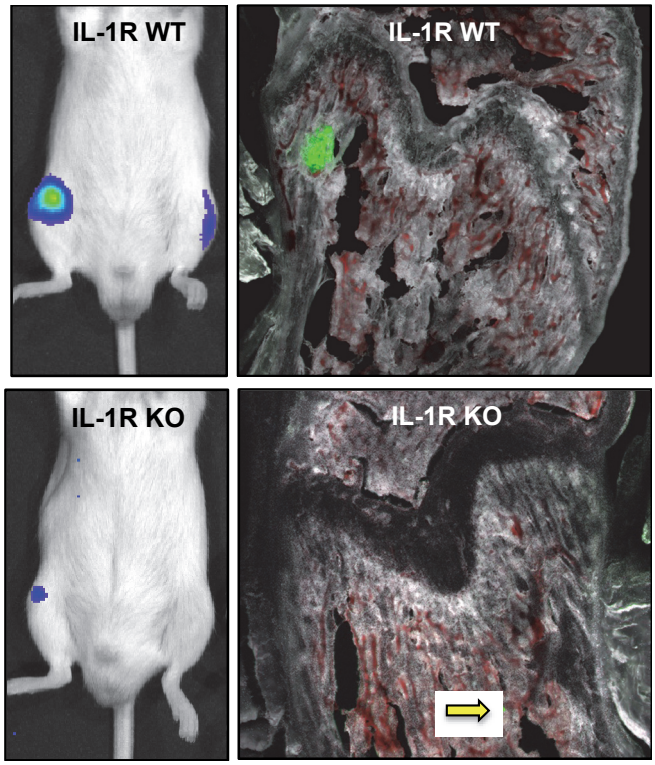

Figure 8: Representative *in vivo* bioluminescence *(left)* and fluorescent micrograph *(right)* images from SCID mice wild-type (WT) or null (KO) for the IL-1R inoculated with PC3-ML cells and sacrificed after two weeks.

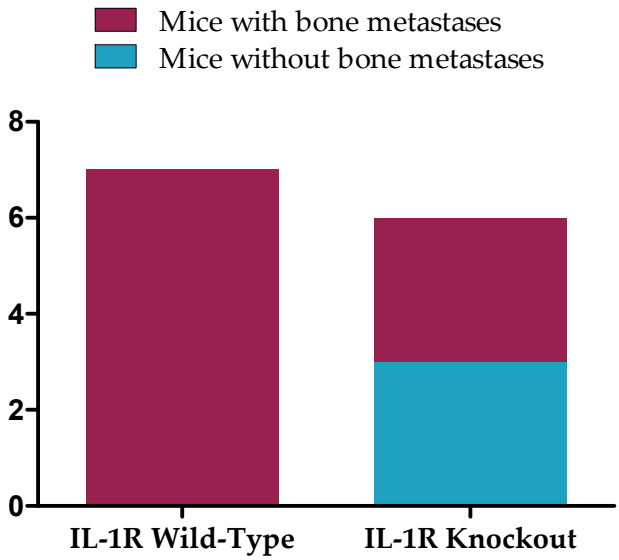

Figure 9: Upon sacrifice, 50% of the IL-1R knockout animals described in *Fig. 8* had no metastatic lesions in the knee joint, while all wild-type animals harbored tumors.

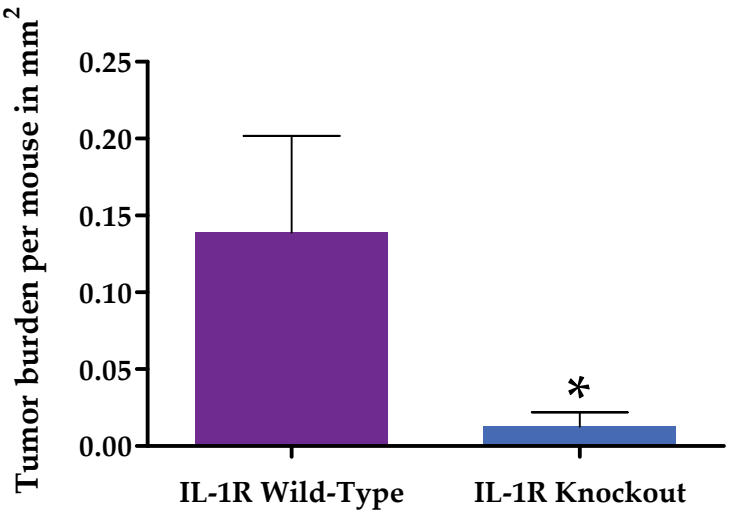

Figure 10: Total PC3-ML tumor burden was significantly reduced in IL-1R KO mice relative to their WT counterparts; this reduction was comparable to 40 mg/kg anakinra and IL-1β knockdown. $p<0.05$.

animal model, and is specifically implicated in the conversion of DTCs into macrometastases [41].

In this chapter, we delved further into the nature of IL-1 signaling in the bone metastatic nice. To begin, we discussed the potent IL-1 antagonist anakinra. Already approved for the treatment of rheumatoid arthritis, this drug has an impressive safety profile despite its status as an immune modulator. The extensive pre- and post-approval analysis support the idea of anakinra as a safe and viable therapeutic, even for cancer patients.

Knowing that IL-1β is only biologically active in its secreted extracellular form, we surmised that a drug such as anakinra would penetrate sufficiently into the bone marrow and there be able to disrupt IL-1β signal transduction. In our preventative model of prostate cancer metastasis, animals inoculated with PC3-ML cells showed a dose-dependent reduction in tumor burden in response to anakinra. This result indicated the great importance of IL-1β signaling during the early stages of metastatic colonization. In the subsequent treatment of established PC3-ML bone lesions with anakinra, the results were indistinguishable from those produced in animals treated with vehicle alone. In this condition we recognize that the critical period for IL-1 activity may have already past, leaving these established tumors to perhaps rely on the activity of osteoclasts *(Fig. 11)* or other IL-1 independent factors for trophic support.

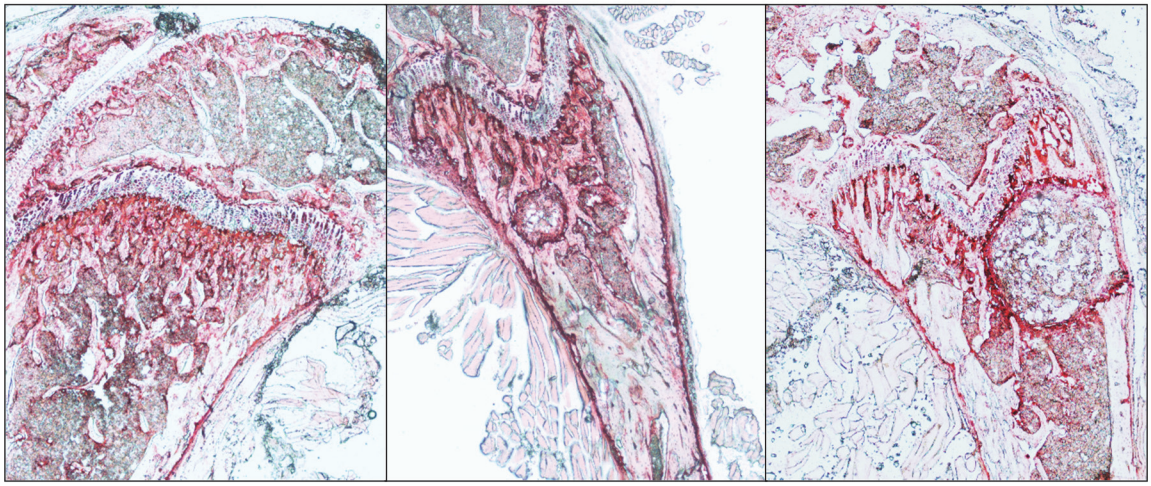

Figure 11: PC3-ML tumors in the distal femurs of SCID mice; TRAP staining of a tumor-free negative control *(left)* reveals a normal distribution of osteoclasts concentrated around the growth plate and endosteum, while lesions are circumscribed by osteoclasts beginning at two weeks *(center)* and persisting beyond three weeks *(bottom right)* post-inoculation.

While the pharmacological blockade of metastatic progression afforded by pre-treatment with anakinra provides additional evidence of the importance of IL-1β in this environment, it cannot distinguish autocrine stimulation by and of cancer cells from paracrine signaling between cancer and resident stromal cells. In order to address this issue, we generated SCID mice with variable expression of the IL-1 receptor. If, as we expected, paracrine communication between DTCs and host tissues was the basis for metastatic progression, then animals null for the IL-1R would bear decreased tumor burden, since their bone stroma would be deaf to provocation by IL-1β. Indeed, not only did the knockout animals produce significantly less tumor volume; in 50% of the IL-1R null animals, no bone metastases could be found at all.

Taken together, these experiments reveal the paracrine nature of the tumor-stromal relationship with regard IL-1β signaling, and present anakinra as a potentially valuable therapeutic tool in the treatment of high-risk or advanced prostate cancer patients. Indeed, this drug could be effective either by preventing the development of bone lesions altogether, or through stabilization of the current number of metastasis by preventing the seeding of additional foci from the primary tumor or another secondary sites, a phenomenon which is now known to be widespread in patients with stage IV disease [61, 62].

Chapter 5: Tumor heterogeneity and the androgen receptor in prostate adenocarcinoma

Androgens as a necessary driver of prostate cancer

The hormonal dependence of PCa is critically exploited in the clinic, with patient care relying heavily on therapeutic strategies that deprive tumor cells of the trophic support supplied by transcriptional activity of the AR. Despite the marked efficacy of initial treatment, androgen-deprivation therapies (ADT) lose the ability to control tumor growth due to the emergence of castration-resistant prostate cancer (CRPC), which is characterized by secondary skeletal lesions and is incurable. In CRPC, various mechanisms allow tumor cells to circumvent ADT, either by mutating the AR to become constitutively active or sensitive to the negligible levels of circulating androgens remaining after gonadal and adrenal blockade, or the local generation of androgens *via* intracrine biosynthetic pathways [63]. Furthermore, point mutations, amplifications, and truncations of the AR that lead to constitutive receptor activation have been proposed as major factors in the unremitting dependence of PCa cells on AR signaling in defiance of treatment-induced selective pressure. Interestingly, it has also been suggested that

PCa cells in both primary and secondary tumors down-regulate AR levels or completely fail to express it [64-66]. However, the presence and proportion of AR− prostate cancer cells in bone metastatic lesions, as established by immunohistochemical approaches, have been repeatedly doubted as artifacts potentially originating from fixation, poor quality of reagents, and flawed methods of quantifying staining intensity [67-69]. Nevertheless, circulating tumor cells (CTCs) collected from CRPC patients show a variable pattern of AR functional signatures when evaluated for prostate specific antigen (PSA) and prostate-specific membrane antigen (PSMA) expression as a downstream readout of AR transcriptional activity [70]. Generally, the absence of AR expression is considered either a feature of a rare variant of PCa characterized by small-cell morphology [71] and Rb loss[72], or the result of neuroendocrine differentiation [73] commonly attributed to hormonal therapies, and which enables a distinct pattern of metastasis to the visceral organs such as the liver and lungs [74, 75]. Only AR-negative cells have been reliably shown to produce bone mets in animal models

Despite the apparent primacy of the androgen receptor in human prostate adenocarcinoma, in our experience intracardiac inoculation of PCa cells into SCID mice results in bone metastatic growth only by a subset of cancer cell lines which are AR-negative; these observations are borne out by the dearth of published

studies showing AR-positive bone metastases in mouse models. This seeming contradiction is particularly troubling given the ongoing doubt in the field regarding the significance, or even existence, of AR-negative cells in PCa metastasis: the prevalence and clinical significance of this phenotype in human disease remains a contested subject [64]. We therefore undertook to definitively characterize these aspects of phenotypic diversity among metastatic prostate cancer cells.

AR-negative cells in human PCa bone metastases

Prostate adenocarcinoma displays considerable intratumoral heterogeneity, a well-established hallmark of many malignancies [76]. Recent studies using deep sequencing of primary and metastatic lesions in patients who succumbed to PCa have revealed patterns of evolution whereby phenotypically distinct subpopulations of cancer cells have been found to coexist at secondary sites [61, 77]. Ultimately, we were able to show that skeletal metastases in PCa patients harbor a considerable fraction of cancer cells lacking AR.

In order to assess the AR status of PCa cells colonizing the skeleton, we examined archival bone biopsies obtained from nine patients in two different clinical cohorts and with documented post-ADT metastatic CRPC. These specimens revealed remarkable variability of AR staining, ranging from lowest to highest signal intensity even within individual lesions *(Fig. 12, arrows)*, while in

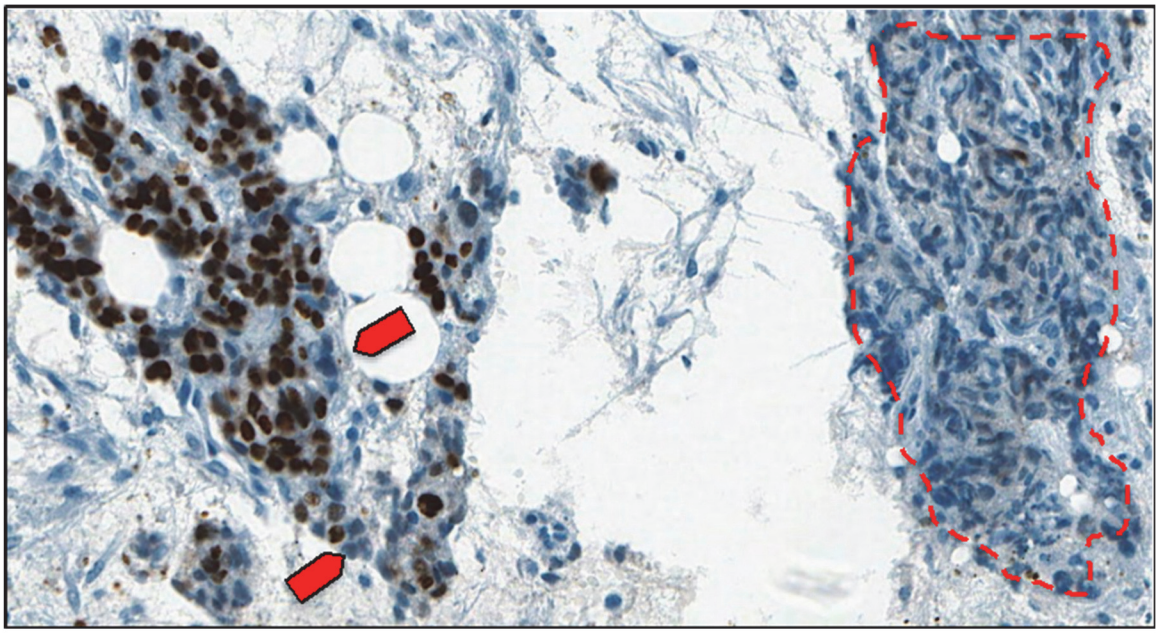

Figure 12: AR expression in skeletal metastases from prostate cancer patients: staining intensity within a single biopsy sample. Cancer cells lacking nuclear AR staining (red arrows) were commonly detected intermixed with AR+ cells; in all specimens, large areas composed almost entirely of cells lacking nuclear AR staining were observed (red dotted line).

some areas the AR could be detected in only a minority of cancer cells *(Fig. 12, dotted line)*. Overall one-third of cancer cells identified by morphological and histopathological criteria in these patients did not stain for AR *(Fig. 13)*. Furthermore, dual immunofluorescence staining with an AR and a pan-cytokeratin antibody [78] confirmed that the cancer cells identified in these metastatic lesions, both with and without AR expression, were indeed of epithelial origin, as can be seen at both primary and bone metastatic sites *(Fig. 14)*.

To provide molecular validation of these findings, we employed Laser Capture Microdissection (LCM) to harvest tissue from the same regions of metastatic tumors examined by IHC staining *(Fig. 15)* and analyzed them by qRT-PCR. The prostatic origin of both AR-positive and AR-negative tumor cells was confirmed by equivalent levels of mRNA for prostein (also known as SLC45A3 or P501S), which is highly restricted to both normal and malignant prostate cells and is routinely used for the diagnosis of metastatic lesions [68, 79, 80]; we were further able to show that the difference in AR status indicated by IHC staining was confirmed at the transcriptional level, providing conclusive evidence that a substantial proportion of PCa cells in bone- metastatic lesions lack AR *(Fig. 16)*. Notably, these cells did not express molecular neuroendocrine (NE) markers such as synaptophysin or chromogranin A *(Table 2)* [81, 82], suggesting that their origin could not be traced either to a primary small-cell carcinoma or to AR+ PCa cells

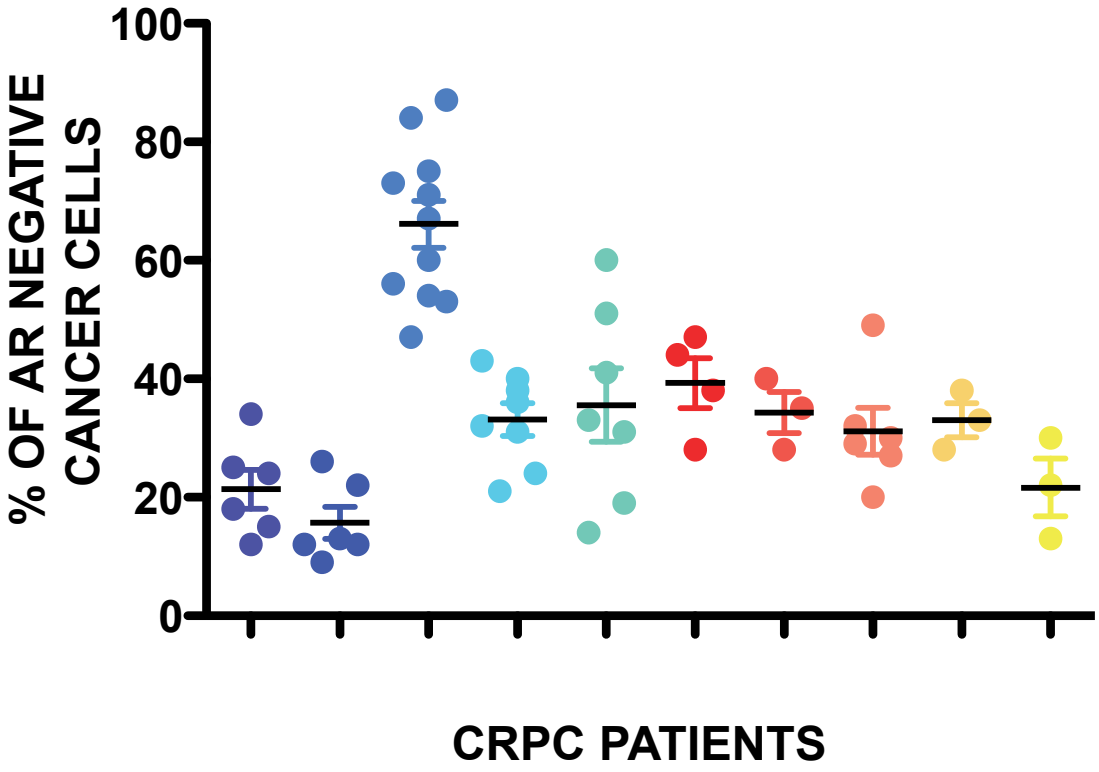

Figure 13: The fraction of prostate cancer cells negative for AR expression detected in bone metastases from ten CRPC patients was found to be 33±14%, with the percentage of infiltrating or resident non-cancerous cells (immune, endothelial or stromal origin) not exceeding 1-2%. Each dot indicates a unique microscopic field of view in which cells were counted.

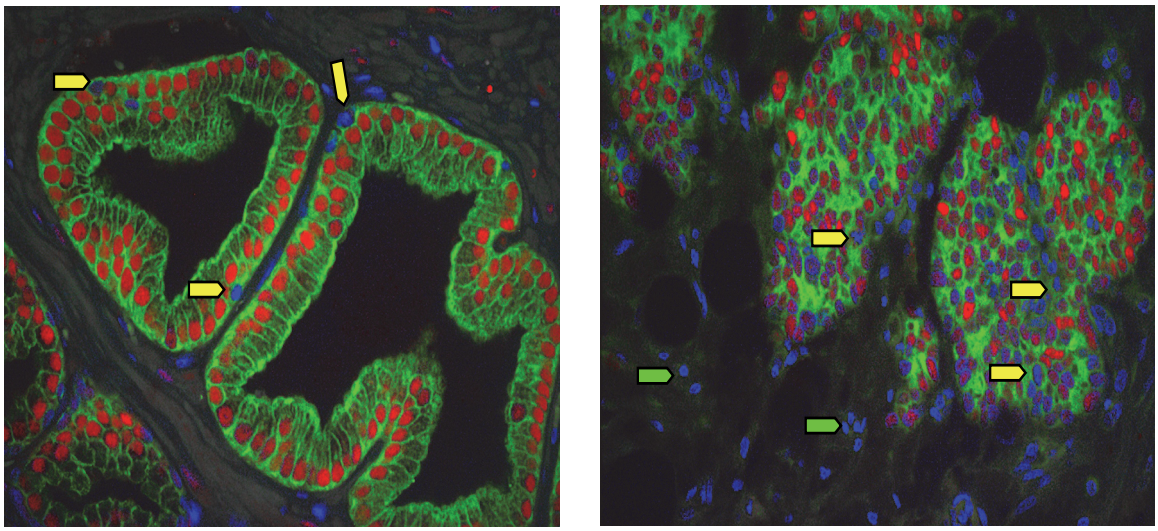

Figure 14: Primary (*left*) and bone metastatic (*right*) tissues stained for pan-cytokeratin (green) and AR (red), with nuclei in blue. These representative images show that both AR+ (red nuclei) and AR− (blue nuclei) cancer cells are of epithelial-derived, and are present in the basal compartment of primary tumors as well as mixed with AR+ cells in skeletal metastases (yellow arrows). Non-epithelial AR− cells were identified in the bone marrow stroma (green arrows).

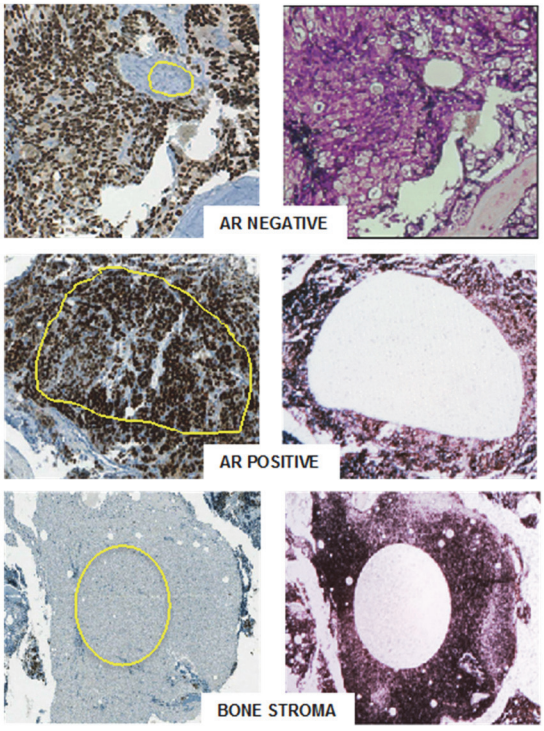

Figure 15: Molecular analysis of tumor and stromal components of human skeletal metastases from prostate cancer patients: tissue samples from areas of tumors lacking (*top*) or highly positive (*middle*) for AR were collected by laser-capture microdissection, as was normal stromal tissue located away from tumor (*bottom*).

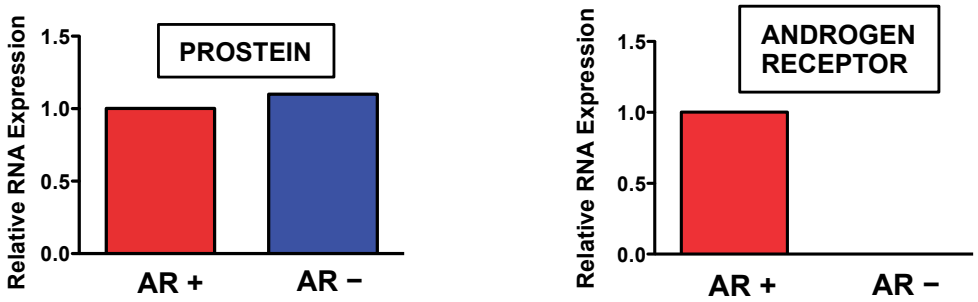

Figure 16: Molecular analysis of tumor and stromal components of human skeletal metastases from prostate cancer patients: qRT-PCR was used to evaluate the expression of the prostate-specific marker prostein, which was detected at comparable levels in prostate cancer cells independently of their AR status, indicating the prostatic origin of both these populations (*left*). The lack of AR expression in cells that stained negative by immunohistochemistry was confirmed at the transcriptional level, providing the first molecular evidence for AR− prostate cancer cells in human skeletal metastases (*right*).

Table 2: Immunohistochemical staining results from the indicated human tissue sample when probed for the neuroendocrine markers synaptophysin and chromogranin A, using cultured mouse neurons as a positive control. While the lung metastasis did stain for both markers as expect, none of the bone samples were positive for either marker regardless of their AR status, indicating that AR-negative prostate cancer cells found in bone metastases are not of the rare neuroendocrine subtype.

SAMPLE	SYNAPTOPHYSIN	CHROMOGRANIN A
MOUSE NEURONAL CULTURE	POSITIVE	POSITIVE
BONE MET #1 [AR +]	NEGATIVE	NEGATIVE
BONE MET #2 [AR+]	NEGATIVE	NEGATIVE
BONE MET #1 [AR −]	NEGATIVE	NEGATIVE
BONE MET #1 [AR −]	NEGATIVE	NEGATIVE
LUNG [AR −]	POSITIVE	POSITIVE

transitioning into an NE phenotype [73, 83]. In contrast, the analysis of a lung metastasis in another patient showed a complete lack of AR associated with expression of NE markers, as is frequently observed in visceral lesions typical of advanced PCa *(Fig. 17)*.

IL-1β and AR expression are mutually exclusive in prostate cancer cells

Interestingly, AR and IL-1β co-expression has not been observed in PCa cells; further, exogenous treatment of AR+ PCa cells with IL-1β peptide has been shown to cause downregulation of the androgen receptor [84, 85].

We first sought to reproduce the existing findings by assessing IL-1β expression in additional human PCa cells either lacking (DU-145) or expressing (LNCaP, VCaP, and 22Rv1) the AR, and found them all to be negative for this cytokine *(Fig. 18)*. All these cells lines failed to metastasize in our model, despite successfully arriving to the skeleton via the arterial circulation and homing as DTCs. This is consistent with our previous work with DU-145 cells [38, 41], as well as the lack of published studies with LNCaP and VCaP cells in pre-clinical models of bone metastasis, and only two existing reports for 22Rv1 cells [86, 87], the results of which could not be reproduced in our hands.

In previous studies, we had observed a negative correlation between PSA immunostaining (as a measure of AR transcriptional activity) and IL-1β expression in bone metastases from a different cohort of patients [41]. Based on these

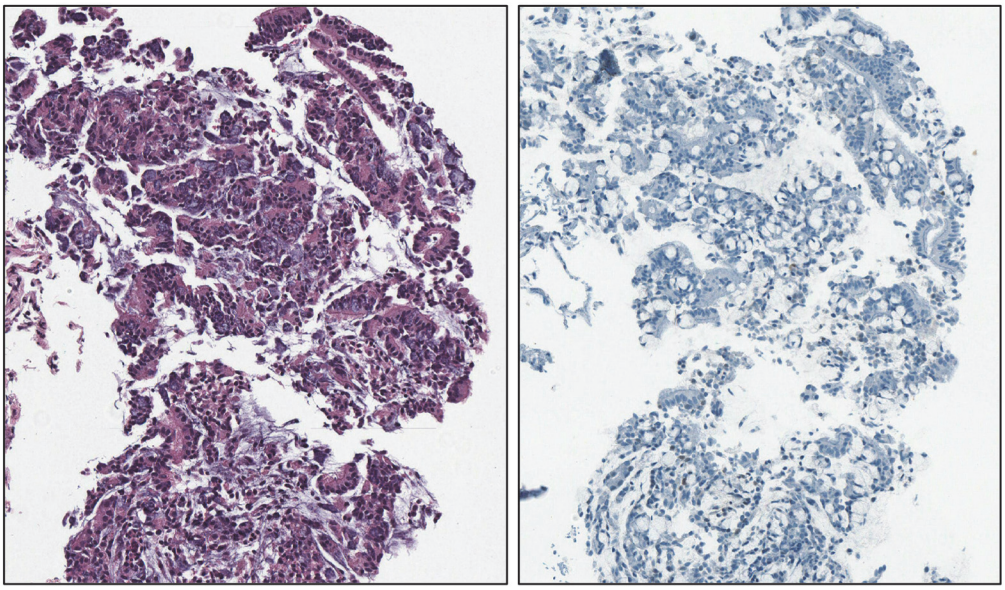

Figure 17: Specimen from a lung metastasis biopsy in a patient with advanced prostate adenocarcinoma, stained with Hematoxylin-Eosin (*left*) and for AR (*right*); a positive control for AR staining may be seen in *Fig. 15*. The absence of AR expression seen here is typical of visceral metastases in these patients.

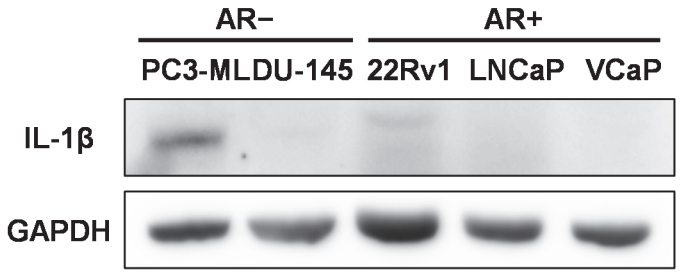

Figure 18: Immunoblot analysis reveals that PC3-ML are the only human prostate cancer cell line tested which endogenously expresses IL-1β.

findings, we further tested the bone metastases from the patients described in the prior section, and found that the AR− prostate cancer cells showed high IL-1β expression, while the AR+ cells tested completely negative for this cytokine. In comparison, the levels of IL-1β transcript detected in bone stroma were significantly lower *(Fig. 19)*. This indicates that PCa cells lacking AR play a dominant role in dictating the local levels of IL-1β during colonization of the skeleton, in contrast to what has been previously proposed by others using subdermal implant of bioengineered scaffolds [88].

Chapter conclusion: heterogeneous cell populations predominate in human disease and may cooperate to enable metastatic progression

The labile nature of the androgen receptor has contributed to the longstanding disagreements over its role and significance in advanced prostate cancer, especially in the situation of CRPC. Alternate biosynthetic pathways for weak androgens notwithstanding, we conclusively show that a substantial segment of the bone metastatic PCa cell population in human patients is negative for the androgen receptor, both on the protein level as detected by IHC, and on the mRNA level as shown through LCM/qRT-PCR. Furthermore, these cells do not express neuroendocrine markers, and so do not represent that small fraction of human disease. These definitive findings establish the AR-negative phenotype as

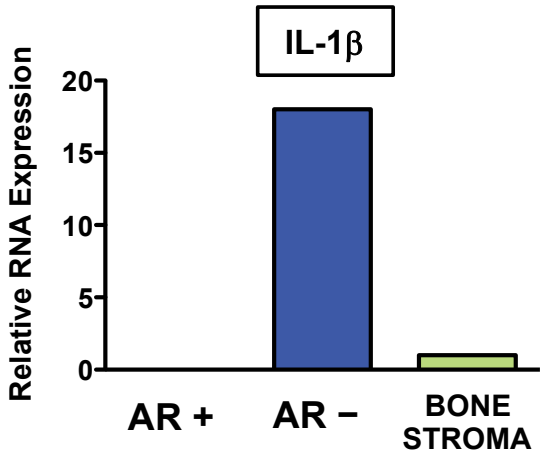

Figure 19: Molecular analysis of tumor and stromal components of human skeletal metastases from prostate cancer patients: IL-1β mRNA was detected exclusively in AR-negative cancer cells, while considerably lower levels were detected in the bone stroma.

a major contributor to most bone metastatic PCa lesions, and one whose influence must be accounted for.

Perhaps even more significantly, by combining the technologies of laser capture of human tissues with quantitative RT-PCR, we were able to establish that AR and IL-1β expression are mutually exclusive among all samples tested. The prominence of androgens in PCa has long been known, while the importance of IL-1β for metastatic progression has been attested by our own work. With these findings in hand, we were led to hypothesize that these two genes, the expression of either of which is hugely beneficial for PCa, are locked in an inherent metabolic conflict which precludes their co-expression from an individual cell. However, their frequent, intimate coexistence in neighboring cells of our patient samples suggest an additional, potentially symbiotic relationship within the metastatic niche, where the pro-metastatic effects induced by each phenotype could, by proximity, also benefit the other. We therefore propose a system of functional tumor heterogeneity existing between AR-negative cells which express IL-1β, and AR-positive cells which do not; together, these two phenotypes may cooperate in order to enable a mutually beneficial colonization of the bone marrow.

Chapter 6: Metastatic cooperation among phenotypically heterogeneous prostate cancer cells

As discussed in the previous chapter, prostate cancer metastases demonstrate a marked phenotypic variety even within an individual lesion [61, 77]. Given the evident and stable diversity of PCa cell populations within individual patients, the possibility that this heterogeneity may be functional and not merely coincidental must be pursued; this is especially true in light of the fact that curative treatments for metastatic PCa remain elusive.

Non-metastatic prostate cancer cell lines

Our discovery of the secreted cytokine IL-1β as a crucial mediator of PCa skeletal metastasis [41] led us to suspect the formation of a pro-metastatic niche in the bone microenvironment; the anti-metastatic effect exerted by anakinra in our animal model, as well as the results from the IL-1R-null animals, further indicate the dependence of AR-negative PCa cells on IL-1β signaling for their metastatic growth. Thus, we surmised that AR−/IL-1β+ cells could also be supportive of indolent cancer cells that, lacking constitutive IL-1β expression, would be incapable of independently generating the molecular crosstalk necessary to

support survival and therefore fail to colonize the bone. This lack of metastasis-forming ability might be offset by the homing of IL-1β-expressing cancer cells to the same site. We therefore postulated that simultaneous injection of AR−/IL-1β+ PC3-ML cells with otherwise non-metastatic cells would enable metastatic progression by both cell types.

Mixed tumors from co-inoculation of metastatic and non-metastatic cell lines

We generated PC3-ML cells stably expressing both the fluorescent protein mCherry and Red Firefly Luciferase, to be paired with the various non-metastatic cell lines, which were engineered to express GFP and Luc2 luciferase. Co-inoculation experiments were then conducted to ascertain whether metastatic PC3-ML cells could support colonization of the skeleton by independently non-metastatic cells in *(Fig. 20)*. We found that this was indeed the case, as mixed tumors could be detected by bioluminescent imaging (BLI) *(Fig. 21)*, as well as through multispectral fluorescence microscopy and x-ray for all cell combinations *(Fig. 22)* starting from the second week post-inoculation. The majority of animals in each study were found to harbor mixed tumors at 4 weeks, as indicated by BLI *(Fig. 23)*, while overall fraction of AR-mixed tumors promoted by PC3-ML cells varied from 59% for LNCaP and 22Rv1 cells to 86% for VCaP *(Fig. 24)*. These results are particularly compelling as they reproduce the scenario observed in skeletal lesions of the PCa patients examined in our study, and overall reflect the

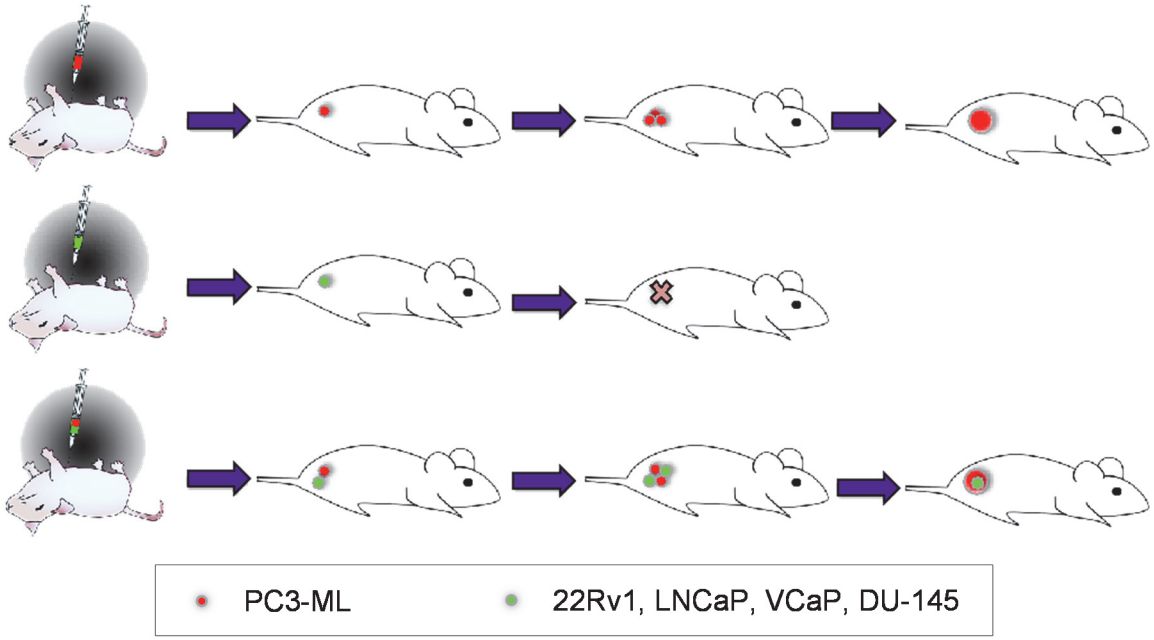

Figure 20: Schematic of experimental design: PC3-ML cells consistently generate skeletal tumors when inoculated in the arterial circulation of mice. These cells were engineered to stably express both the mCherry red-fluorescent protein and Red Firefly Luciferase (RedLuc)*(top)*. In contrast, 22Rv1, LNCaP, VCaP and DU-145, engineered to stably expressing GFP and Luc2 luciferase, are capable of disseminating to the skeleton but fail to colonize the bone and grow into tumor foci *(middle)*. Given the stromal effects of IL-1β, we proposed that co-inoculation of metastatic and non-metastatic cells would produce mixed lesions *(bottom)*.

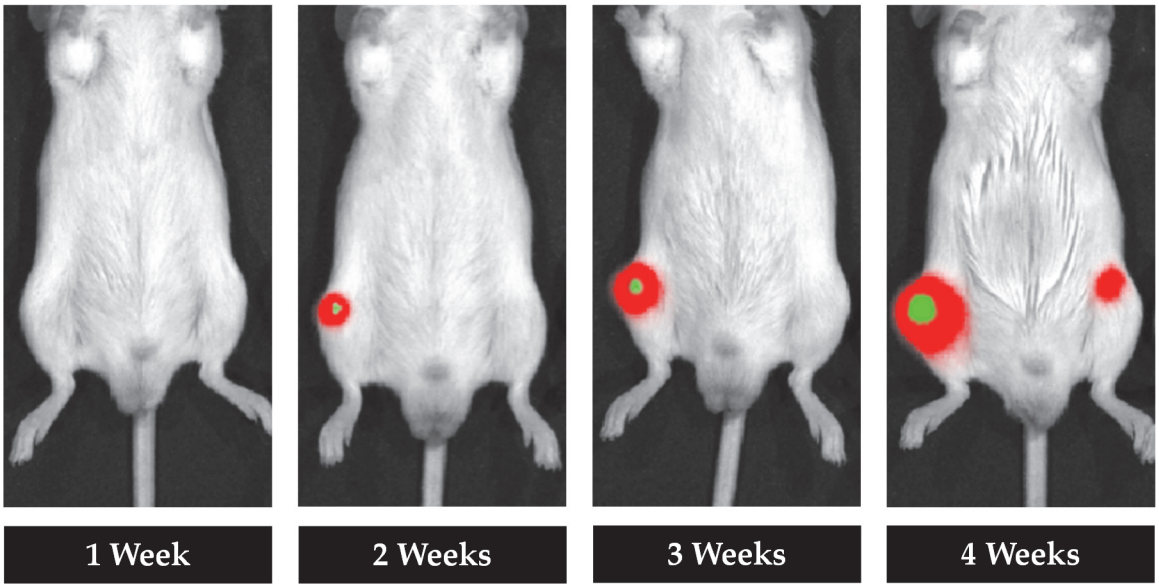

Figure 21: Cancer cell cooperation in the bone metastatic niche: non-metastatic cancer cell lines (green) generated bone tumors when co-inoculated with PC3-ML cells (red), as shown by weekly bioluminescent imaging of the same individual using filters to distinguish RedLuc and Luc2.

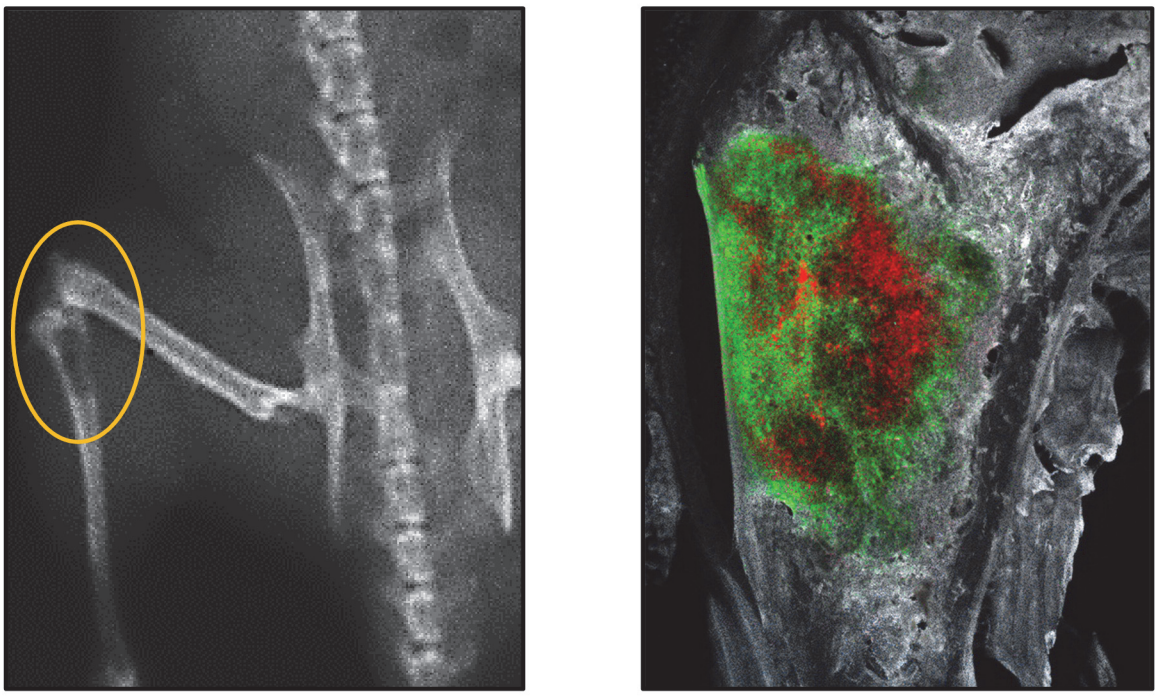

Figure 22: Cancer cell cooperation in the bone metastatic niche: mixed tumors induce skeletal alterations revealed by x-ray (*left*); upon sacrifice, the bones positive for bioluminescent signals were inspected by multispectral fluorescence microscopy. The detection of both red and green fluorescent signals indicated that tumors were comprised of both prostate cancer cell lines (*right*). Unfortunately, due to the design features of our multispectral imaging system, it is not possible to accurately overlay a two-spectrum image; when inspected by eye through a fluorescent microscope, these lesions reveal large yellow areas in which the two cell types are thoroughly intermixed.

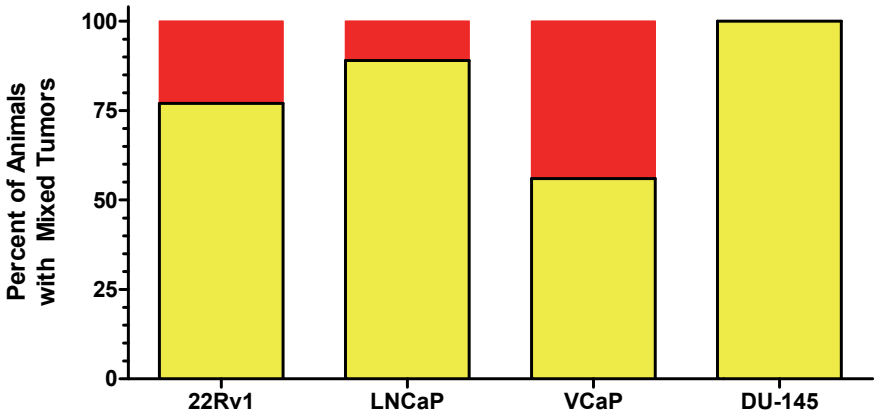

Figure 23: Cancer cell cooperation in the bone metastatic niche: mixed bone metastases were reliably produced in the majority of animals co-inoculated with PC3-ML cells and the indicated non-metastatic cell line, with yellow indicating the percentage of mice injected which developed mixed metastatic lesions, and determined by dual-color BLI.

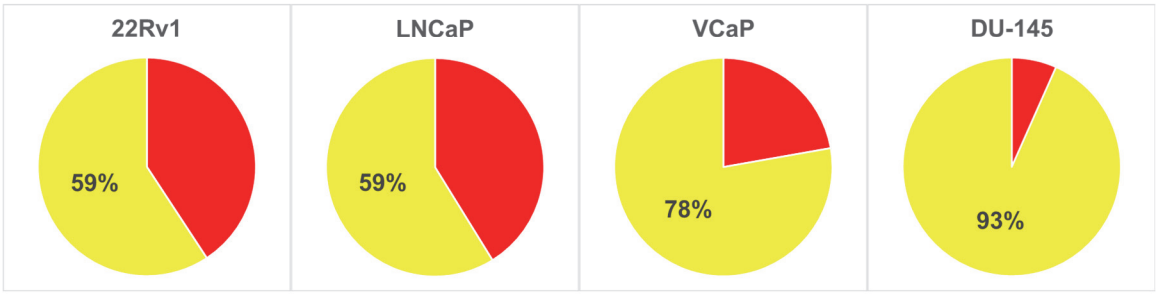

Figure 24: Cancer cell cooperation in the bone metastatic niche: the percentage of mixed tumors detected by bioluminescence in inoculated mice varied with each cell combination, ranging from 59% for PC3-ML+LNCaP or 22RV1 to 93% for PC3-ML+DU-145.

widely-reported genetic, hormonal, and likely functional heterogeneity of cancer cells in human metastases [89, 90]. Interestingly, AR+ cancer cells appeared to benefit significantly more from the presence of PC3-ML cells in terms of relative tumor size than did the AR− DU-145 cells *(Fig. 25)*; further studies will be required to determine whether this reflects a possible increase in AR transcriptional activity promoted by locally secreted IL-1β.

Metastatic cooperation between cancer cells is tissue-specific and an early event

Next, we sought to discern whether the cooperation among cancer cells revealed by the experiments described above is an early event, or one that takes time to be established. To dissect the earliest stages of metastasis, we examined the bones of animals sacrificed five minutes and 24 hours after intracardiac co-inoculation of PC3-ML cells and a non-metastatic cell line.

For the experiments in which animals were sacrificed five minutes after inoculation, the presence or absence of PC3-ML cells proved immaterial: non-metastatic cells were both found to populate the bone in large numbers regardless of whether they had been injected alongside PC3-ML cells *(Fig. 26)*. While not indicating any particular role for IL-1β at this time point, these results do further support the conclusion that even non-metastatic PCa cells arrive in the bone marrow efficiently in early stages post-inoculation. More interestingly, in the case

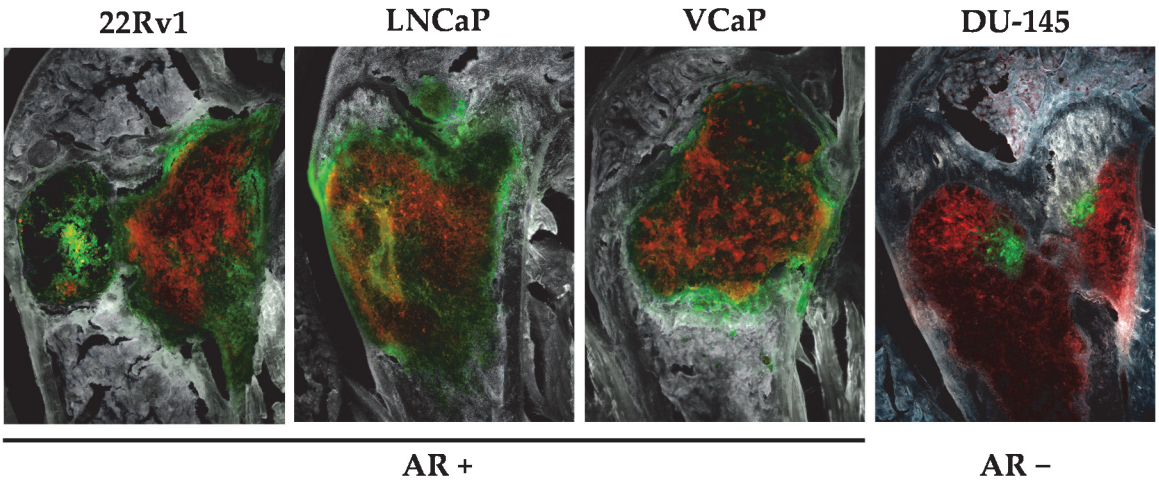

Figure 25: Cancer cell cooperation in the bone metastatic niche: the three AR+ cancer cell types appear to comprise half of tumor area when co-inoculated with PC3-ML, while AR− DU-145 cells contribute considerably less.

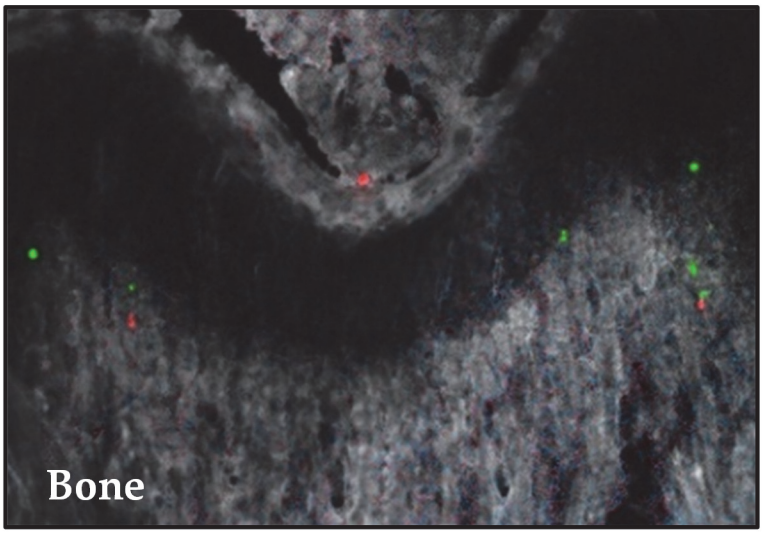

Figure 26: Cooperation between metastatic and non-metastatic prostate cancer cells is an early event: tibiae and femora of mice grafted in the systemic blood circulation with fluorescent cancer cells were collected 24 hours post-inoculation, processed for cryosectioning and inspected for DTCs by multispectral fluorescence microscopy. In co-inoculation experiments, both highly metastatic PC3-ML cells (red) and independently non-metastatic cancer cells (green) were detected predominantly near the epiphyseal growth plate.

of the animals sacrificed after 24 hours, the knee joints revealed that the presence of PC3-ML cells led to a significant increase in the number of otherwise non-metastatic 22Rv1 and VCaP cells found in the skeleton, compared to unaccompanied inoculation of these cells *(Fig. 27)*. Together, these findings support a pro-metastatic role for IL-1β, which begins almost immediately after the initial lodging of cancer cells in the skeleton and leads to critical changes in the bone microenvironment during the first 24 hours of metastatic dissemination.

Additionally, we sought to determine the tissue specificity of this phenomenon. Upon examination of the lungs of the animals injected for 24 hours with either VCaP cells alone or VCaP in conjugation with PC3-ML, we revealed the cooperative effect to be specific to the bone microenvironment, as no difference in colonization by VCaP cells was observed in these animals *(Fig. 28)*. As subsequent data will suggest, this intriguing finding may be due to the differences in the stromal cells which exist in each tissue type: in the bone, mesenchymal stem cells are the dominant component, while in the lung more terminally-differentiated myofibroblasts and pericytes predominate [91].

Cell cooperation is driven by IL-1β

These findings were further strengthened by experiments using the non-metastatic and AR-negative DU-145 cell line engineered to stably express high levels of IL-1β *(Fig. 29)*, which we have previously shown to impart them with *de*

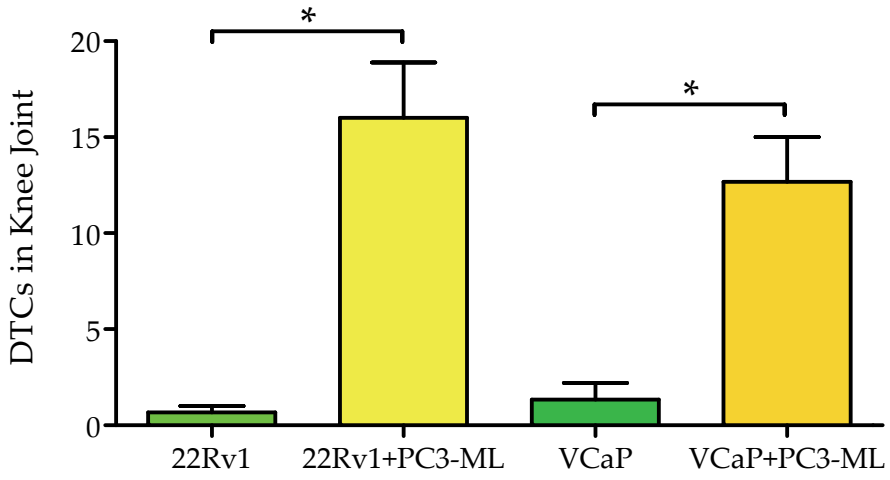

Figure 27: Cooperation between metastatic and non-metastatic prostate cancer cells is an early event: co-inoculation with PC3-ML cells dramatically increased the number of 22Rv1 or VCaP that lodged to the bone after 24 hours compared to these cell types inoculated alone. Results are shown as the mean ± s.e.m (3 mice per group). *$p < 0.05$ Magnification: 200x

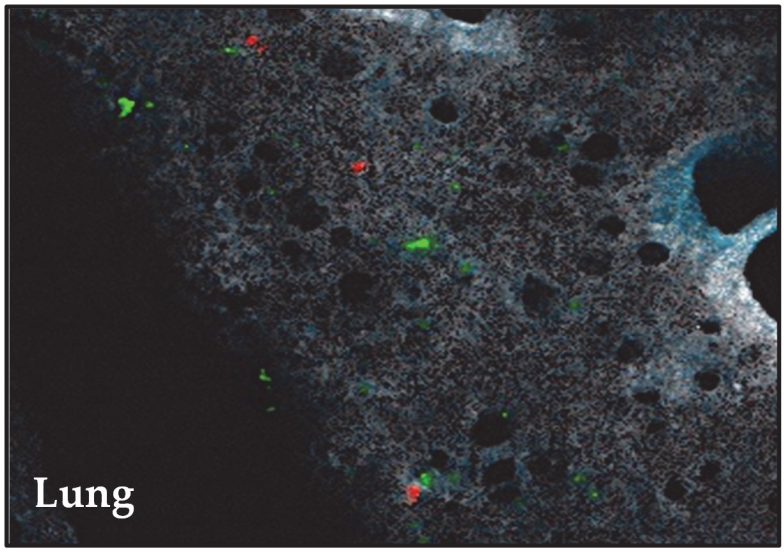

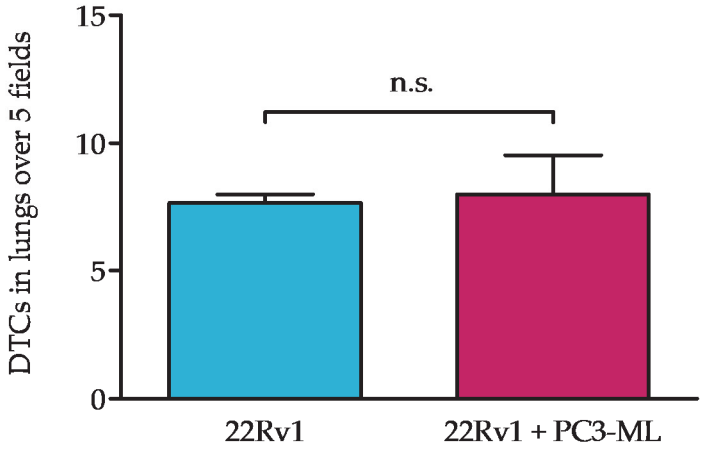

Figure 28: The supportive effect exerted by PC3-ML cells is specific to the bone marrow microenvironment and was not observed in lung: when this tissue was examined for DTCs across 5 randomly selected microscopic fields, the number of 22Rv1 cells detected 24 hours post-inoculation was independent of co-inoculation of PC3-ML cells.

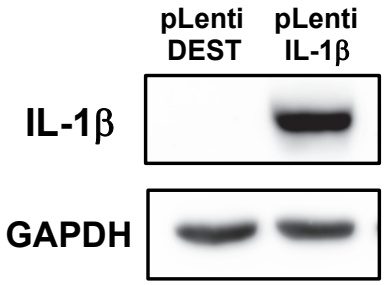

Figure 29: Immunoblot showing DU-145 cells made to express high levels of IL-1β using a selectable lentiviral vector.

novo metastatic ability [41]. These cells were labeled with mCherry and co-injected with GFP-labeled VCaP cells and the mice sacrificed after 24 hours. Upon examination of their femora and tibiae, we again found a significant increase in the arrival of VCaP cells relative to their solitary inoculation *(Fig. 30, left)*, indicating that both PC3-ML cells and DU-145 cells exogenously expressing IL-1β enable bone colonization by non-metastatic cells. Furthermore, long-term studies using DU-145(IL-1β) cells co-inoculated with VCaP also resulted in the formation of mixed metastatic lesions *(Fig. 30, right)*. When considered in sum, these findings recapitulate our observations of skeletal metastases from advanced prostate cancer patients: dissemination of PCa cells with the AR−/IL-1β phenotype promotes bone colonization by independently non-metastatic AR+ PCa cells.

Chapter conclusion: IL-1β drives cancer cell cooperation in the bone metastatic niche

In this segment, we began by testing our hypothesis of cooperative metastatic colonization by phenotypically distinct prostate cancer cell populations. First, we confirmed the inability of non-IL-1β-expressing cells to metastasize in our animal model. Next, we paired each of four non-metastatic cell lines with PC3-MLs for simultaneous injections, and were able to consistently produce large bone metastases consisting of both cell types. These mixed metastases were anatomically and biologically extremely similar to those found in

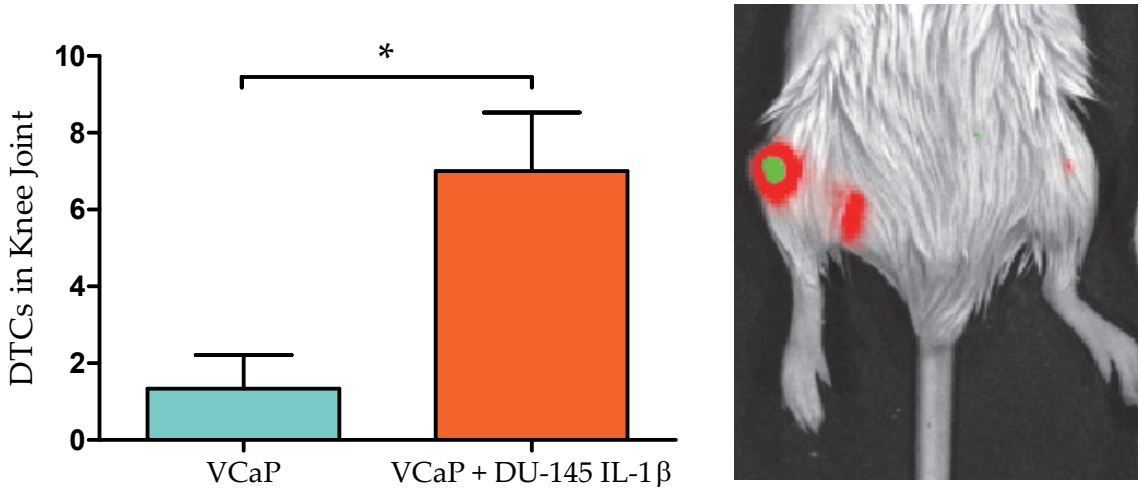

Figure 30: IL-1β drives cell cooperation: VCaP cells colonize the bone more efficiently at 24 hours when co-inoculated with DU-145 cells over-expressing IL-1β (*left*); long-term studies using animals co-inoculated with VCaP (green) and DU-145 IL-1β (red) cells reveal the formation of mixed bone metastases by BLI (*right*). *$p < 0.05$

the human patient samples analyzed in Chapter 5, and their existence supports our contention of biochemical cooperation between distinct cancer cell populations: AR-positive cells, incapable of metastasizing or producing IL-1β on their own, can nevertheless contribute to large, aggressive metastatic lesions when co-inoculated with PC3-ML cells.

In order to better understand the phenomenon of cell cooperation, we performed short-term studies in which disseminated tumor cells were quantified under various conditions. In accounting for DTCs in the knee joints, we found that all of our cell lines were present in the bone in large numbers five minutes post-inoculation, regardless of their ultimate metastatic potential. However, when DTCs were assessed 24 hours after injection, we found that the non-metastatic cells were nearly absent when they had been inoculated alone, while these same cells persisted in great numbers in the presence of PC3-MLs. Furthermore, when the lungs of the animals from these studies were evaluated for DTCs, we found no difference in the number of non-metastatic cells at 24 hours whether they had been injected alone or in combination with PC3-ML cells, indicating that the cooperation effect is specific to the bone. We were thus able to conclude that a critical step in cell cooperation occurs within the first 24 hours in the skeleton, where otherwise non-metastatic cells are able to colonize and remain in the bone microenvironment. However, we did not yet possess conclusive evidence that IL-

1β was the causative factor enabling cell cooperation; as stated in Chapter 1, two additional genes were found to be upregulated in metastatic PCa cells, and it could have been one of those, or something else entirely, which was responsible for cooperation. We therefore engineered the non-metastatic AR-negative and IL-1β-negative DU-145 cell line to express high levels of IL-1β, then co-inoculated these with non-metastatic VCaP cells. At both 24 hours and multiple weeks we again saw evidence of cell cooperation, with VCaP cells persisting and developing in concert with DU-145(IL-1β) cells to form large mixed lesions. Based on these findings, we can confidently conclude that the secreted cytokine IL-1β produced by some PCa cells is capable of founding a metastatic niche, enabling the emergency of large, heterogeneous lesions in the bone.

Chapter 7: Interleukin-1β induces phenotypic changes in the bone stroma which support metastatic progression

Responses of prostate cancer cells to direct stimulation with IL-1β

While the data presented in the previous chapter confirmed the importance of IL-1β in the bone-metastatic niche, we had yet to fully understand the trajectory of the crucial IL-1 signaling. To this end, we assayed the various PCa cell lines used in this study for expression of the IL-1R in order to determine their potential receptivity to paracrine IL-1β signaling, and found the receptor present in each *(Fig. 31)*. However, exposure to IL-1β peptide *in vitro* revealed a varying profile of signal transduction among AR+ PCa cell lines that benefited equally from PC3-ML cells when colonizing the bone, suggesting that paracrine stimulation *via* IL-1R is unlike to be primarily responsible for the metastatic cell cooperation we observed *(Fig. 32)*. On the other hand, human bone Mesenchymal Stem Cells (hMSCs), which are an abundant component of the bone stroma, when similarly exposed to IL-1β exhibited a rapid and sustained signaling response, indicating definite susceptibility to this cytokine *(Fig. 33)*.

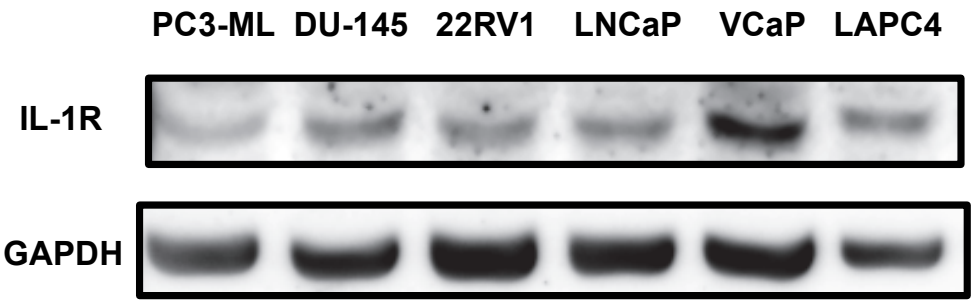

Figure 31: Prostate cancer cell lines exhibit varying responses to direct stimulation with IL-1β: expression of the IL-1 receptor varies considerably across PCa cell lines.

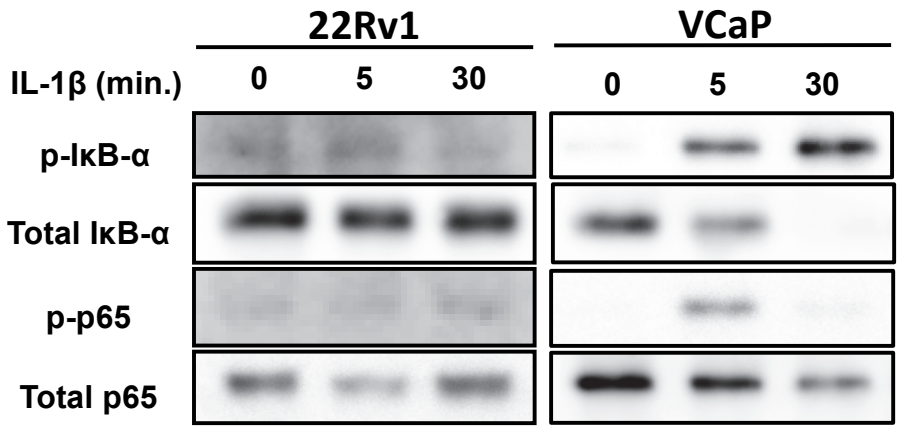

Figure 32: Prostate cancer cell lines exhibit varying responses to direct stimulation with IL-1β: 22Rv1 and VCaP cells, despite benefiting equally from co-existence with IL-1β producing PC3-ML cells at the skeletal level, showed divergent signaling in response to exogenous treatment with the cytokine.

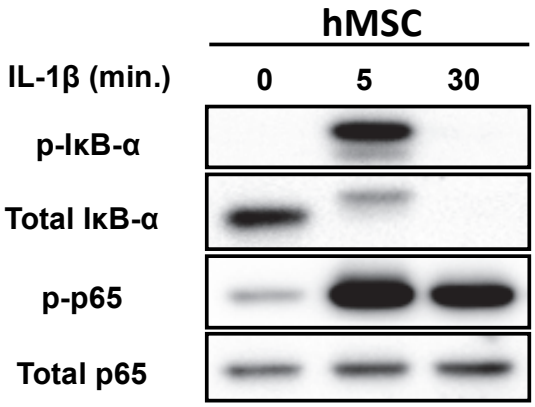

Figure 33: hMSCs responded to IL-1β stimulation with a strong activation of the canonical NF-κB pathway.

IL-1β phenotypically alters resident bone stromal cells *in vitro*

In our prior publication establishing the role of IL-1β in PCa metastasis, we showed that IL-1β secreted by metastatic PC3-ML cells specifically upregulated cyclooxygenase-2 (COX-2) expression in both hMSCs and human osteoclasts [41]. The phenotypic change that this cytokine was able to induce in these two major components of the skeletal stroma indicated to us the possibility that IL-1β acts as a potent mediator of the bone microenvironment, perhaps influencing the "soil" of the BME to become receptive to the "seeds" of disseminated PCa cells [92].

In the past decade, the tumor microenvironment and interactions between cancer and stromal cells have become the focus of a great deal of research. Non-neoplastic fibroblasts are now known to play a role in the progression of a wide variety of tumors, both at primary and secondary sites [93]. Carcinoma-associated fibroblasts (CAFs) are those mesenchymally-derived cells which, under the influence of cancer cells, have evolved to aid in malignant development despite having no tumorigenic capacity themselves [94]. CAFs are a heterogeneous population with diverse protein expression, but S100A4 (also known as fibroblast specific protein-1, FSP-1) has emerged as the most definitive CAF marker [95].

The dependence of normal prostate epithelium on supportive stroma has long been known, and the symbiotic relationship between PCa and reactive stroma

was established more than a decade ago [25]. Pro-inflammatory cytokines such as TGF-β and IL-8 have been recognized as important mediators of these interactions, particularly for metastatic cells in the BME. However, anti-inflammatory therapies have not proven effective against PCa metastasis [24]. Our data points to the specific role of IL-1β in the influence of metastatic PCa cells on the bone stroma, and the differentiation of MSCs into CAFs. The studies proposed here will further elucidate this interaction, including molecular characterization of the reciprocation by CAFs to IL-1β-secreting PCa cells. Similarly, much recent research has emphasized the unique features of tumor-initiating cells (TICs), a sub-population of cancer cells which are independently capable of establishing either primary or secondary lesions [36, 96]. Established tumors display a diverse population of constituent malignant cells; it remains an open question whether TICs are cancer stem cells, which themselves differentiate into a complete tumor, or if they are cells capable of inducing a receptive pro-metastatic niche which then supports the growth of other cancer cells of various phenotypes. The phenomenon of cancer cell cooperation described here recapitulates the clinical finding of mixed-phenotype tumors, and suggests the latter: metastatic IL-1β-secreting PCa cells support the growth of non-metastatic, non-IL-1β-secreting PCa cells

Having thus identified the stroma as a key driver of IL-1β-mediated metastasis, we sought to further explore its activity during skeletal metastatic

progression. We exposed hMSCs in vitro for one week to IL-1β peptide (25 pg/mL) or CM from PC3-ML cells, then examined for morphological and biochemical markers indicating their conversion to CAFs [97]. CAFs have a well-established role in primary tumors [98, 99] and are widely thought to act similarly at secondary sites. We found that hMSCs responded to IL-1β by formation of elongated actin stress fibers, suggestive of a transition into CAFs [100]; a similar change in morphology was generated by CM from PC3-ML cells, which are known to secrete IL-1β [41]. In either case, the effect observed was abrogated by inclusion of anakinra in the culture medium *(Fig. 34)*. Consistent with this finding, the expression of the CAF-marker S100A4 (also known as FSP1) increased in hMSCs exposed to either IL-1β peptide or CM from PC3-ML cells, an effect which again was blocked by anakinra *(Fig. 35)*.

IL-1β induces CAF-like differentiation of bone stromal cells *in vivo*

In light of these *in vitro* findings, we proceeded to determine whether the stroma surrounding skeletal metastases in our animal model responded to tumor-secreted IL-1β in a similar fashion. Bone stroma immediately adjacent to and some distance away from tumors generated by PC3-ML cells was harvested by LCM from IL-1R wild-type mice *(Fig. 36, left)*; in the same animals, stroma from bones which did not harbor any tumors was also collected *(Fig. 36, center)*; as were analogous samples from IL-1R knockout mice *(Fig. 36, right)*. RNA was isolated

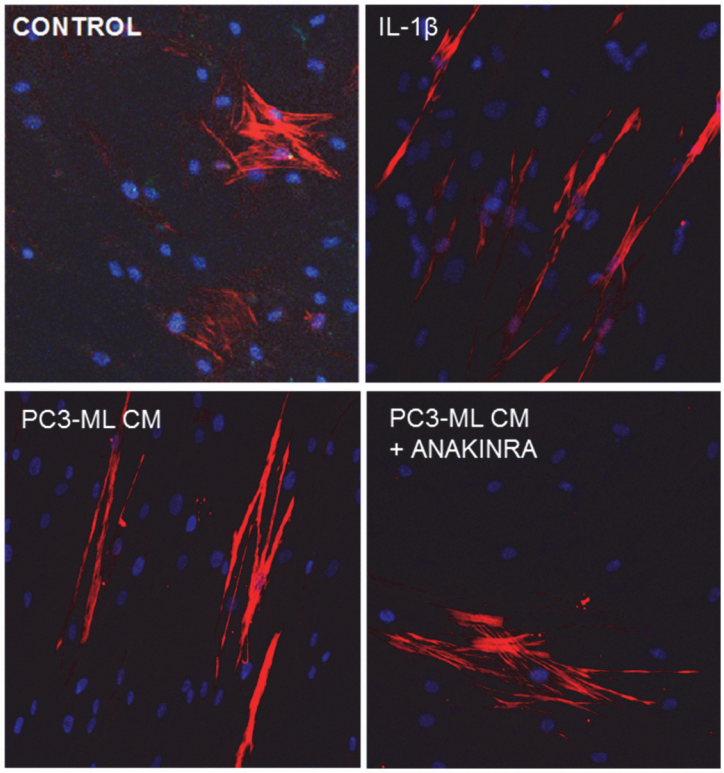

Figure 34: Human mesenchymal stem cells (hMSCs) were treated for one week with regular media, recombinant human IL-1β peptide (25 pg/mL), or PC3-ML cell conditioned media (PC3-ML CM) with and without anakinra (10 μg/mL). They were then stained for α-smooth muscle actin (red) and DAPI (blue), revealing stress fibers in response to IL-1β (25pg/ml) and PC3-ML CM that were eliminated with anakinra (10μg/ml). CM= Conditioned Media

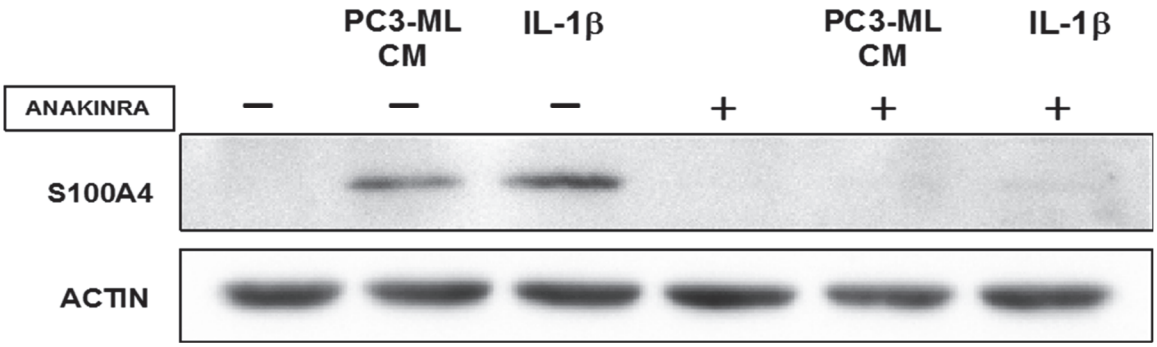

Figure 35: hMSCs treated as in *Fig. 34* were lysed and subjected to western blotting for actin and the CAF marker S100A4; S100A4 was found to be upregulated in response to IL-1β and PC3-ML CM, an effect which was fully abrogated in the presence of anakinra.

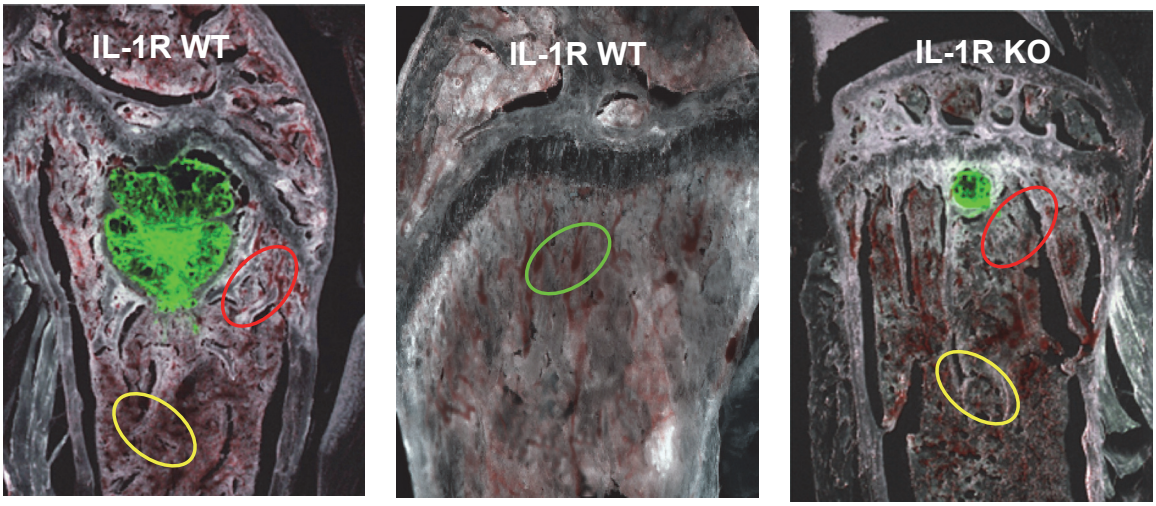

Figure 36: SCID mice wild-type (WT) and null (KO) for IL-1R were inoculated with fluorescently-labeled PC3-ML human prostate cancer cells and sacrificed after three weeks, with the resulting tissue subjected to LCM of stromal regions adjacent to tumors (red), distant from tumors (yellow), and from tumor-free bones (green).

from these samples and subjected to qRT-PCR against Cyclooxygenase-2 (COX-2) and the CAF marker S100A4, as both molecules are known to be induced in stromal cells by exposure to IL-1β [36, 41], and S100A4 expression would indicate the development of CAFs in the metastatic niche [101]. By this analysis we were able to show that both COX-2 and S100A4 were significantly upregulated in the tumor-adjacent stroma derived from IL-1R WT animals, with a relative expression level between WT and KO of about 7-fold for COX-2 and more than 100-fold for S100A4. This effect appeared spatially delimited: stroma located some distance from tumors was only minimally affected, likely due to the concentration gradient of IL-1β secreted by the cancer cells. Further, in IL-1R knockout animals the expression of stromal S100A4 and COX-2 was totally unaffected by the presence of tumors, confirming the causal role of IL-1 signaling in this process *(Fig. 37)*. These findings fully recapitulate those derived in vitro and strongly suggest that highly metastatic PCa cells such as PC3-ML condition the bone tissue by producing IL-1β, which induces the reprogramming of hMSCs to a CAF-like phenotype. This then changes the local microenvironment into a metastatic niche highly permissive of the survival and growth of disseminated tumor cells (DTCs), increasing the likelihood of metastatic progression.

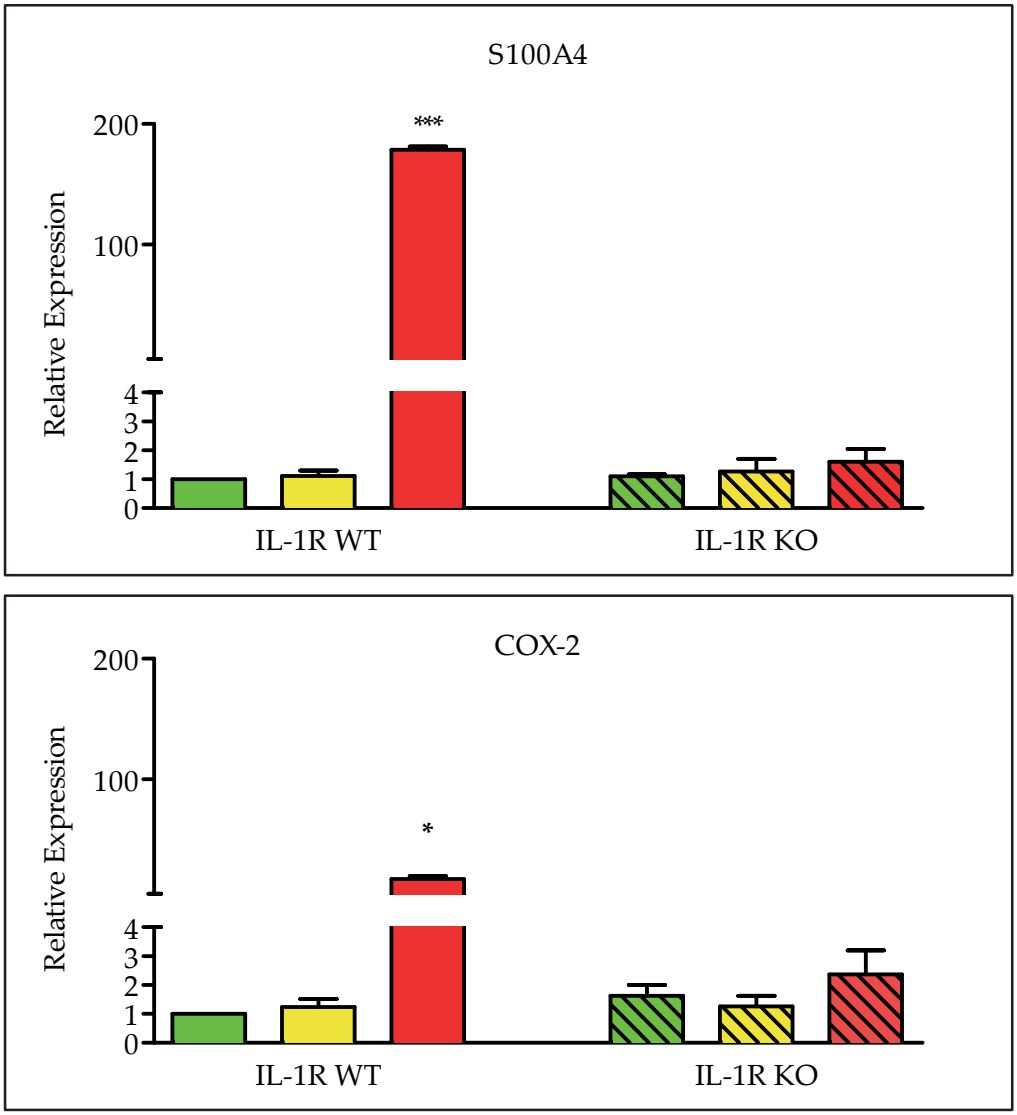

Figure 37: IL-1β induces CAF-like differentiation of bone stromal cells *in vivo*: Upon qRT-PCR analysis of the LCM samples shown in *Fig. 36*, S100A4 (*top*) and the IL-1β downstream target COX-2 (*bottom*) were specifically upregulated at the mRNA level exclusively in tumor-associated stroma of WT animals, indicating a local effect dependent on IL-1β signaling.

Gene expression profiling of LCM stoma samples

The growth-permissive niche generated by IL-1β likely involves alterations in local concentrations of molecular mediators produced by cells either naturally inhabiting the bone stroma or migrating to the tumor-colonized tissue microenvironment. With the intent of identify specific genes altered by IL-1β signaling in tumor-associated bone stromal cells, we interrogated the same LCM tissue specimens analyzed above for S100A4 and COX-2 expression by using Nanostring technology and an nCounter panel of 750 genes with established relevance in adaptive, humoral, and innate immune response as well as inflammation. We detected 30 genes for which expression was significantly altered two folds or more by the presence of prostate cancer cells as compared to bone stroma either free of tumors or harvested from IL-1R KO animals *(Table 3)(Fig. 38).*

Finally, our gene profiling studies identify alterations in mediators of tumor growth and progression affecting the bone stroma within the metastatic niche. In addition to confirming the up-regulation of *COX-2* previously detected by qRT-PCR, we found that the up-regulation of Integrins α1, β2 and β4, Osteopontin, Tumor Necrosis Factor (TNF) 13 (TNF13 or BAFF) and TNF receptor 17 *(Fig. 39)* both corroborates earlier studies by others [102-104] and delineates a profile of pro-tumorigenic genes regulated by IL-1β secreted from metastasis-initiating cells. Equally compelling is the 7-fold down-regulation of interleukin-24 (IL-24), a

Table 3: Genes either up- or down-regulated by at least 2-fold in tumor-associated bone stroma from IL-1R WT SCID mice bearing PC3-ML bone metastases for three weeks; genes showing alteration by 3-fold or more are labeled with darker color hues.

Gene name	Accession Number	Fold change	*p* Value	
Abcb1a	NM_011076.1	4.82	0.0026	Multidrug resistance protein 1
Angpt1	NM_009640.3	3.66	0.01	Angiopoietin
Ccl5	NM_013653.3	3.53	0.0375	Chemokine
Itgb2	NM_008404.4	3.25	0.0093	Integrin beta 2
Ptgs2	NM_011198.3	3.21	0.0058	COX-2
Cfh	NM_009888.3	2.89	0.0299	Regulator of complement activation
Spp1	NM_009263.3	2.81	0.0049	Osteopontin
Birc5	NM_009689.2	2.72	0.0405	IAP member
Itga1	NM_001033228.3	2.69	0.0186	Integrin alpha 1
Tnfrsf17	NM_011608.1	2.62	0.039	TNF receptor – binds TNF13b
Fos	NM_010234.2	2.43	0.0432	Oncogene
Vim	NM_011701.4	2.28	0.0211	Vimentin
Tnfsf13b	NM_033622.1	2.17	0.0085	TNF13b
Itgb4	NM_001005608.2	2.16	0.0449	Integrin beta 4
Dusp6	NM_026268.2	2.01	0.0085	Dual specific phosphatase 6
H2-Dma	NM_010386.3	-2	0.0125	Histocompatibility 2, class II, locus DMa
Ecsit	NM_001253897.1	-2.06	0.0488	Signaling integrator
Thbs1	NM_011580.3	-2.16	0.0362	Trombospondin 1
Cxcl5	NM_009141.2	-2.17	0.0135	Chemokine
Mcam	NM_023061.2	-2.37	0.0195	Melanoma cell adhesion molecule
Cd34	NM_001111059.1	-2.39	0.0068	Cell surface glycoprotein
Trp53	NM_011640.1	-2.5	0.018	Tumor suppressor
C1ra	NM_023143.3	-2.51	0.0205	Complement component 1r
Tfeb	NM_001161723.1	-3.08	0.0046	Transcription factor EB
Masp2	NM_010767.3	-3.21	0.0357	Mannan-binding Lectin Serine Peptidase 2
Cdh1	NM_009864.2	-3.3	0.0326	Cadherin 1
Hspb2	NM_024441.3	-3.44	0.0132	Heat shock protein 2
Cd74	NM_001042605.1	-4.01	0.0249	Major histocompatibility complex, class II
C1s1	NM_144938.2	-6.09	0.0095	Complement component 1, subcomp. 1
Il24	NM_053095.2	-6.86	0.0165	Interleukin 24

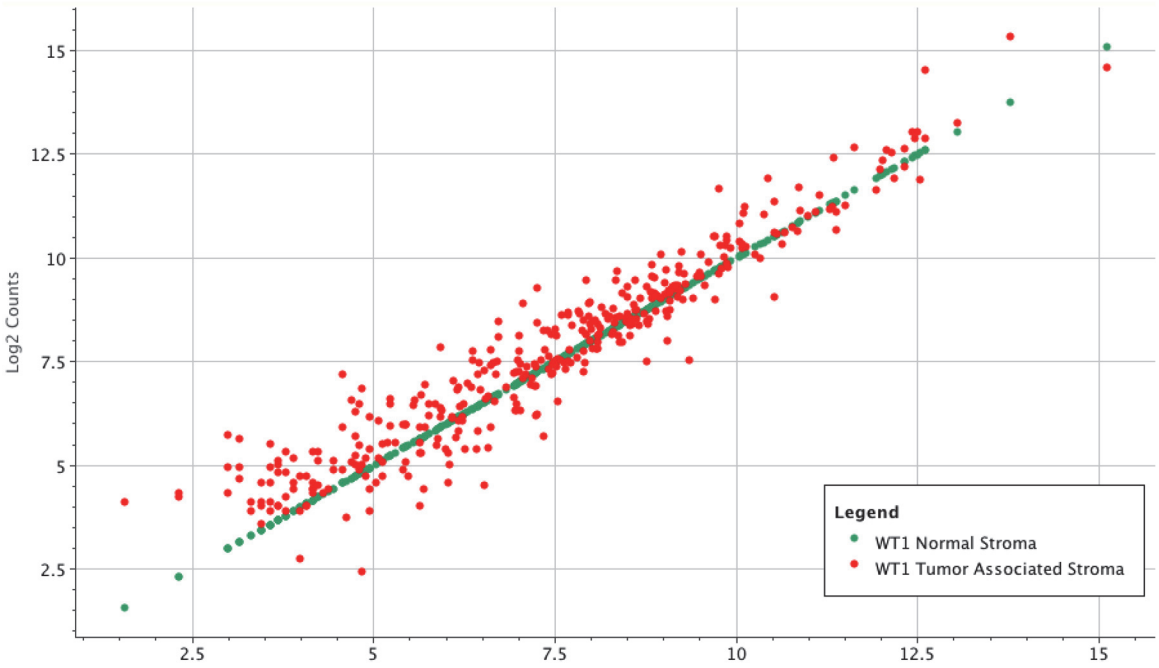

Figure 38: Transcriptome analysis by Nanostring technology shows genes altered in the bone stroma by the presence of prostate cancer cells (red) as compared to bone stroma either free of tumors (green) or associated to tumors in IL-1R KO animals. Among the 750 genes analyzed, we identified 30 genes for which expression was significantly altered by two fold or more.

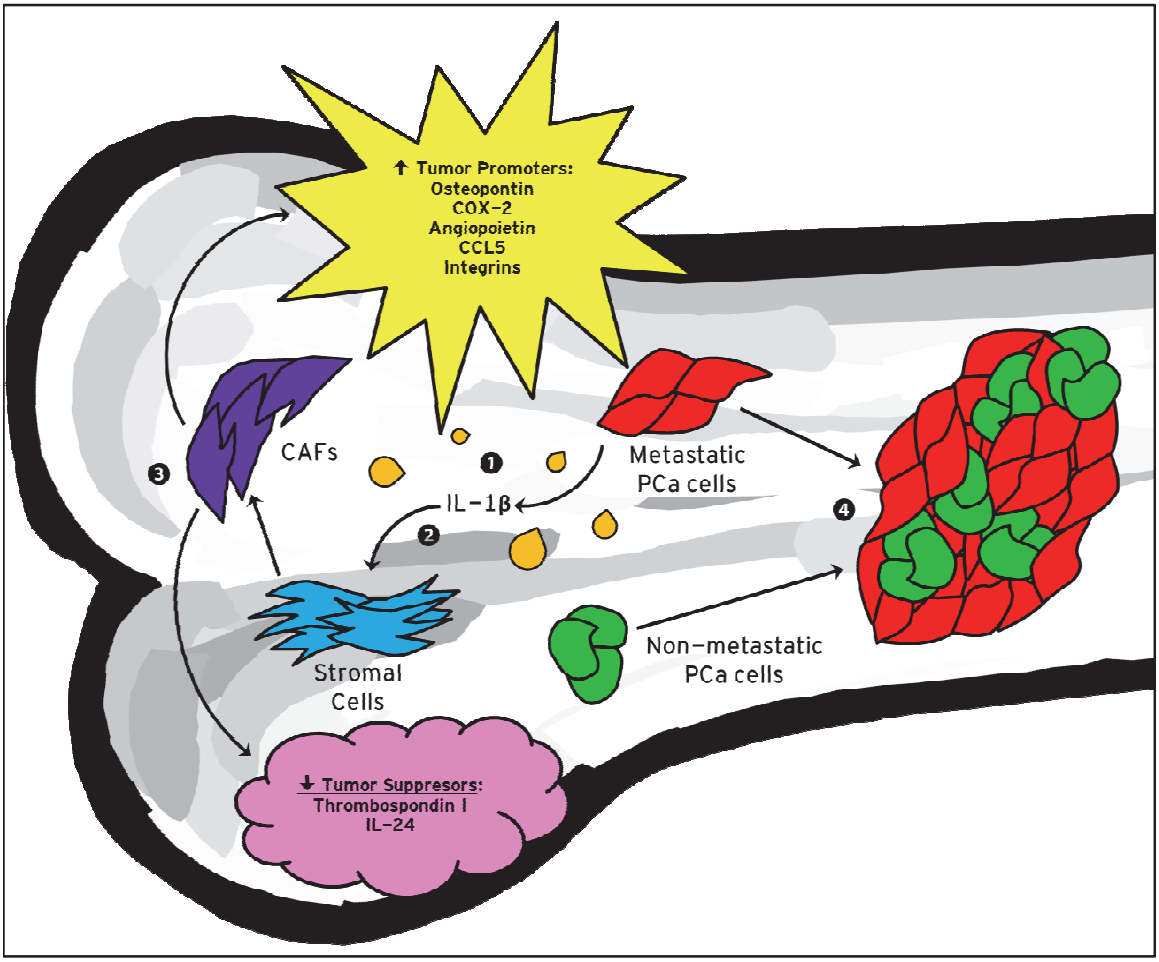

Figure 39: We propose a novel model of the bone metastatic niche in which metastatic prostate cancer cells lacking the androgen receptor (*red*) achieve a metastasis-initiating role by secreting IL-1β (1), causing the transition of mesenchymal stem cells into CAFs (2). The tumor-supporting role of CAFs is likely exerted through the upregulation of tumor promoters and the downregulation of tumor suppressors (3), generating a local microenvironment which favors colonization and growth by cancer cells regardless of their individual metastatic phenotype (*green*); this sequence of events leads to metastatic tumors consisting of AR-mixed populations of cancer cells (4).

cytokine with a pleiotropic tumor-suppressing role that involves decreasing stemness of human prostate cancer cells [105], which supports the need for lessening its expression during tumor colonization of the metastatic niche. On the same line, down-regulation of two initiating components of the Complement cascade (C1r and C1s) and of mannan-binding lectin serine peptidase 2 (Masp2) [106] inevitably hints to an impairment of the innate immune-response, which has been proposed to control tumor growth *via* several types of immune cells including NK cells [107, 108]. As NK cells are normally present in immune-compromised SCID mice, which were used in our study, these results delineate a conceivable scenario in which tumor-derived IL-1β mitigates the killing of cancer cells by innate immune response in the bone microenvironment.

Chapter conclusion: Cancer cell-derived IL-1β molecularly alters the bone microenvironment, permitting metastatic colonization by a diverse cohort of PCa cells

In this final set of experiments, we have seen how the IL-1β produced by metastatic AR-negative prostate cancer cells is capable of influencing the bone stroma in a way which favors the development of bone metastases. First, we interrogated our panel of cell lines for their response to direct stimulation with IL-1β; the range of responses found across the group indicated that it was unlikely that direct stimulation was the means through which IL-1β enables cell

cooperation. We therefore shifted our attention to the resident stromal cells of the bone microenvironment, where we not only confirmed our previous findings regarding the sensitivity of hMSCs to IL-1β [41], but identified specific changes in these cells resulting in a carcinoma-associated fibroblast phenotype *in vitro*.

The ultimate significance of the stromal response to cancer cell-derived IL-1β was revealed by molecular analysis of LCM stroma samples derived from IL-1R SCID mice. Quantification of the IL-1 target COX-2 and the CAF marker S100A4 confirmed the *in vitro* findings, with only wild-type IL-1R animals inducing the gene expression changes *in vivo*. Taking advantage of this circumstance, we used Nanostring analysis of these stromal samples to identify downstream effects of IL-1 signaling. Of the more than 30 genes whose expression was altered by at least two fold, downregulation of the tumor suppressors thrombospondin 1 and interleukin-24 and upregulation of the putative tumor promotors osteopontin, COX-2, angiopoetin, CCL5, and various integrins are of particular interest. Given the striking effect which stromal IL-1R status has on the ability of PCa cells to form metastases, we offer these genes as potential therapeutic targets of a new category of drugs which aim to control prostate cancer bone metastasis through disruption of cancer cell cooperation.

Chapter 8: Discussion and suggested studies

Prostate cancer cells growing as skeletal metastases are thought to strictly depend on AR activation by androgens either circulating or produced locally by cancer cells, even upon emergence of the advanced castration-resistant form of the disease. Consequently, the treatments currently available for CRPC patients rely heavily on pharmacologic approaches that impair AR transcriptional activity. However, while anti-androgens can afford an increase in overall survival, targeting the AR has so far failed to provide a curative resolution for these patients. This suggests the existence of an additional tumor-promoting mechanism, which supports metastatic progression at the skeletal level; a better understanding of the complex functional interactions between disseminated cancer cells and the surrounding microenvironment promises to reveal new therapeutic targets.

In this study, we demonstrate by molecular means that a considerable proportion of the cells in bone metastatic lesions from PCa patients do not express AR. These cells did not express NE markers and therefore differ from those frequently detected in visceral metastases typical of the advanced disease. This suggests that PCa patients harbor multiple AR− phenotypes with distinct organ-

tropism or that a NE-conversion of AR− cancer cells follows their dissemination to soft-tissues. Furthermore, we reveal an inverse relationship between AR and IL-1β expression in these cell populations, which in animal models translates to the restriction of the aggressive bone-metastatic behavior exclusively to AR−/IL-1β+ phenotypes. IL-1β is associated with tumor-promoting effects [52-54], but its function in metastases has been proposed mostly from circumstantial evidence [55]. Here, we show that PCa cells fail to progress beyond the stage of isolated DTCs when surrounded by unconditioned stroma; they can colonize and grow in the bone only when inhabiting an IL-1β-conditioned tissue microenvironment.

Based on these findings, we believe that AR− PCa cells that simultaneously secrete IL-1β are instrumental in setting the stage for colonization and metastatic progression in the skeleton. At the same time, these cells are inevitably bound to evade the restraint on growth and survival exerted by AR antagonists. More detailed studies will be necessary to ascertain whether AR−/IL-1β+ cells are implicated in promoting, at least in part, the resistance to AR-antagonists that frequently emerges in AR+ PCa cells during ADT [109, 110]. Regardless, treatment strategies which aim to directly impair the substantial AR− cellular component of skeletal metastatic lesions in CRPC patients should be seriously considered. For instance, drugs disrupting the functional interactions of IL-1β with IL-1R could be

combined with AR antagonists with the ultimate intent of effectively addressing the heterogeneous AR status of the PCa cells growing at the skeletal level.

This study also underlines the potential role of COX-2 and other stromal factors downstream of IL-1β stimulation as mediators of skeletal colonization by PCa cells. In the current study, molecular analysis of tumor-associated mouse stroma revealed the tumor suppressors Thrombospondin-1 and IL-24, and the tumor promotors osteopontin, angiopoietin, CCL5, and several integrins to be down- and up-regulated, respectively. Moreover, while the expression of COX-2 was initially used in this study as a functional read-out for bone stroma activation by IL-1β, compounds targeting this enzyme have shown anti-metastatic effects in pre-clinical breast and colon cancer models [111]; the data presented here may in fact provide the mechanistic basis for understanding this effect. Based on this information, therapies targeting each of these proteins should be seriously considered in the context of CRPC.

Collectively, the results shown here describe and characterize a previously unknown functional heterogeneity in metastatic prostate cancer and provide a strong incentive for the clinical testing of pharmacological agents targeting IL-1β signaling, either as a standalone approach or in combination with the current standard of care.

LIST OF REFERENCES

LIST OF REFERENCES

1. Mann, T.R.R., *The Biochemistry of Semen*. 1954, London: Methuen & Co. Ltd. 240.

2. Ross, A.E. and R. Rodriguez, *Development, Molecular Biology, and Physiology of the Prostate*, in *Campbell-Walsh Urology*, A.J. Wein, et al., Editors. 2015, Elsevier: Philadelphia, PA. p. 2393-2424.

3. Nelson, W.G., et al., *Prostate Cancer*, in *Abeloff's Clinical Oncology*, J.O. Armitage, et al., Editors. 2014, Saunders Elsevier: Philadelphia, PA. p. 1463-1496.

4. Rohr, H. and G. Bartsch, *Human benign prostatic hyperplasia: a stromal disease? New perspectives by quantitative morphology.* Urology, 1980. **16**(6): p. 625-633.

5. Epstein, J.I. and T.L. Lotan, *The Lower Urinary Tract and Male Genital System*, in *Robbins and Cotran Pathologic Basis of Disease*, V. Kumar, A.K. Abbas, and J.C. Aster, Editors. 2015, Saunders Elsevier. p. 959-990.

6. *SEER Stat Fact Sheets: Prostate Cancer*. 2016 [cited 2016 May 13]; Available from: http://seer.cancer.gov/statfacts/html/prost.html.

7. Howlader N, N.A., Krapcho M, Garshell J, Neyman N, Altekruse SF, Kosary CL, Yu M, Ruhl J, Tatalovich Z, Cho H, Mariotto A, Lewis DR, Chen HS, Feuer EJ, Cronin KA *SEER Cancer Statistics Review, 1975-2010*. 2013.

8. Jain, S., et al., *Diagnosis and Management of Cancer Using Serologic and Other Body Fluid Markers*, in *Henry's clinical diagnosis and management by laboratory methods*, R.A. McPherson and M.R. Pincus, Editors. 2017, Elsevier: St. Louis, MO. p. 1432-1449.

9. Carter, H.B., et al., *Early detection of prostate cancer: AUA guideline.* The Journal of urology, 2013. **190**(2): p. 419-426.

10. Bubendorf, L., et al., *Metastatic patterns of prostate cancer: An autopsy study of 1,589 patients.* Human Pathology, 2000. **31**(5): p. 578-583.

11. Rizzo, S.S., *Prostate epithelial stem cells.* Cell proliferation. **38**(6): p. 363-374.

12. Toivanen, R., A. Mohan, and M.M. Shen, *Basal Progenitors Contribute to Repair of the Prostate Epithelium Following Induced Luminal Anoikis.* Stem cell reports, 2016. **6**(5): p. 660-667.

13. Epstein, J.I., *Pathology of Prostatic Neoplasia*, in *Campbell-Walsh Urology*, A.J. Wein, et al., Editors. 2015, Elsevier: Philadelphia, PA. p. 2593-2600.

14. Lee, S.H.S.H., *Cell types of origin for prostate cancer.* Current opinion in cell biology. **37**: p. 35-41.

15. Priemer, D.S.D.S., *Neuroendocrine Tumors of the Prostate: Emerging Insights from Molecular Data and Updates to the 2016 World Health Organization Classification.* Endocrine pathology. **27**(2): p. 123-135.

16. *AJCC Cancer Staging Manual*. 7th ed. 2010, New York: Springer-Verlag New York.

17. Gleason, D.F. and G.T. Mellinger, *Prediction of prognosis for prostatic adenocarcinoma by combined histological grading and clinical staging.* The Journal of Urology, 1974. **111**(1): p. 58-64.

18. Moyer, V.A., *Screening for prostate cancer: US Preventive Services Task Force recommendation statement.* Annals of internal medicine, 2012. **157**(2): p. 120-134.

19. Nørgaard, M., et al., *Skeletal related events, bone metastasis and survival of prostate cancer: a population based cohort study in Denmark (1999 to 2007).* The Journal of urology, 2010. **184**(1): p. 162-167.

20. Rove, K.O. and E.D. Crawford, *Evolution of Treatment Options for Patients With CRPC and Bone Metastases: Bone-Targeted Agents That Go Beyond Palliation of Symptoms to Improve Overall Survival.* ONCOLOGY, 2011. **25**(14).

21. Wang, C. and Y. Shen, *Study on the distribution features of bone metastases in prostate cancer.* Nuclear Medicine Communications, 2012. **33**(4): p. 379-383.

22. Kricun, M.E., *Red-yellow marrow conversion: its effect on the location of some solitary bone lesions.* Skeletal radiology, 1985. **14**(1): p. 10-19.

23. Morgan, J.W., K.A. Adcock, and R.E. Donohue, *Distribution of skeletal metastases in prostatic and lung cancer: Mechanisms of skeletal metastases.* Urology, 1990. **36**(1): p. 31-34.

24. Suva, L.J., et al., *Bone metastasis: mechanisms and therapeutic opportunities.* Nature Reviews Endocrinology, 2011. **7**(4): p. 208-218.

25. Chung, L.W., *Prostate carcinoma bone-stroma interaction and its biologic and therapeutic implications.* Cancer, 2003. **97**(S3): p. 772-778.

26. Ferlay, J., et al., *Cancer incidence and mortality worldwide: sources, methods and major patterns in GLOBOCAN 2012.* International journal of cancer, 2015. **136**(5): p. E359-E386.

27. Alva, A. and M. Hussain, *The Changing Natural History of Metastatic Prostate Cancer.* The Cancer Journal, 2013. **19**(1): p. 19-24.

28. Grabowska, M.M., et al., *Mouse models of prostate cancer: picking the best model for the question.* Cancer and Metastasis Reviews, 2014. **33**: p. 377-397.

29. Hensley, P.J. and N. Kyprianou, *Modeling prostate cancer in mice: limitations and opportunities.* Journal of andrology, 2012. **33**(2): p. 133-144.

30. Jung, J., *Human tumor xenograft models for preclinical assessment of anticancer drug development.* Toxicological Res, 2014. **30**(1): p. 1-5.

31. Khanna, C. and K. Hunter, *Modeling metastasis in vivo.* Carcinogenesis, 2005. **26**(3): p. 513-523.

32. Jamieson-Gladney, W.L., et al., *The chemokine receptor CX 3 CR1 is directly involved in the arrest of breast cancer cells to the skeleton.* Breast Cancer Research, 2011. **13**(5): p. 1.

33. Russell, M.R., et al., *The α-receptor for platelet-derived growth factor confers bone-metastatic potential to prostate cancer cells by ligand-and dimerization-independent mechanisms.* Cancer research, 2010. **70**(10): p. 4195-4203.

34. Purton, L.E. and D.T. Scadden, *The hematopoietic stem cell niche.* 2008.

35. Wang, M. and M.E. Stearns, *Isolation and characterization of PC-3 human prostatic tumor sublines which preferentially metastasize to select organs in SCID mice.* Differentiation, 1991. **48**(2): p. 115-125.

36. Li, H.-J., et al., *Cancer-stimulated mesenchymal stem cells create a carcinoma stem cell niche via prostaglandin E2 signaling.* Cancer discovery, 2012. **2**(9): p. 840-855.

37. Kaighn, M., et al., *Establishment and characterization of a human prostatic carcinoma cell line (PC-3).* Investigative urology, 1979. **17**(1): p. 16-23.

38. Russell, M., et al., *The α-receptor for platelet-derived growth factor as a target for antibody-mediated inhibition of skeletal metastases from prostate cancer cells.* Oncogene, 2008. **28**(3): p. 412-421.

39. Dolloff, N.G., et al., *Bone-metastatic potential of human prostate cancer cells correlates with Akt/PKB activation by α platelet-derived growth factor receptor.* Oncogene, 2005. **24**(45): p. 6848-6854.

40. Stone, K.R., et al., *Isolation of a human prostate carcinoma cell line (DU 145).* International journal of cancer, 1978. **21**(3): p. 274-281.

41. Liu, Q., et al., *Interleukin-1β Promotes Skeletal Colonization and Progression of Metastatic Prostate Cancer Cells with Neuroendocrine Features.* Cancer research, 2013. **73**(11): p. 3297-3305.

42. Charles, A., *Interleukin-l and Its Biologically Related Cytokines.* Advances in immunology, 1989. **44**: p. 153.

43. Dinarello, C.A., *The interleukin-1 family: 10 years of discovery.* The FASEB Journal, 1994. **8**(15): p. 1314-1325.

44. Weber, A., P. Wasiliew, and M. Kracht, *Interleukin-1 (IL-1) pathway.* Science signaling, 2010. **3**(105): p. cm1.

45. Hannum, C.H., et al., *Interleukin-1 receptor antagonist activity of a human interleukin-1 inhibitor.* Nature, 1990. **343**(6256): p. 336-340.

46. Arend, W.P., et al., *Biological properties of recombinant human monocyte-derived interleukin 1 receptor antagonist.* Journal of Clinical Investigation, 1990. **85**(5): p. 1694.

47. Seckinger, P., et al., *Natural and recombinant human IL-1 receptor antagonists block the effects of IL-1 on bone resorption and prostaglandin production.* The Journal of Immunology, 1990. **145**(12): p. 4181-4184.

48. Hannum, C.H., et al., *Interleukin-1 inhibitors*. 1993, Google Patents.

49. Sabados, B.K., *Pharmaceutical formulations of interleukin-1 inhibitors*. 2008, Google Patents.

50. *USAN Council. List No. 366. New names. Anakinra.* Clin Pharmacol Ther, 1994. **56**(5): p. 592.

51. Siegel, J.P., *Product Approval Information - Licensing Action BL 103950/0 (Anakinra)*, O.o.T.R.a. Review and C.f.B.E.a. Research, Editors. 2001: Rockville, MD.

52. Voronov, E., et al., *IL-1 is required for tumor invasiveness and angiogenesis.* Proceedings of the National Academy of Sciences, 2003. **100**(5): p. 2645-2650.

53. Lewis, A.M., et al., *Interleukin-1 and cancer progression: the emerging role of interleukin-1 receptor antagonist as a novel therapeutic agent in cancer treatment.* Journal of translational medicine, 2006. **4**(1): p. 1.

54. Valdivia-Silva, J.E., et al., *Effect of pro-inflammatory cytokine stimulation on human breast cancer: implications of chemokine receptor expression in cancer metastasis.* Cancer letters, 2009. **283**(2): p. 176-185.

55. Dinarello, C.A., *Why not treat human cancer with interleukin-1 blockade?* Cancer and Metastasis Reviews, 2010. **29**(2): p. 317-329.

56. Oliveira, A., et al., *Interleukin-1β genotype and circulating levels in cancer patients: metastatic status and pain perception.* Clinical biochemistry, 2014. **47**(13): p. 1209-1213.

57. Yin, J., et al., *Activation of the RalGEF/Ral pathway promotes prostate cancer metastasis to bone.* Molecular and cellular biology, 2007. **27**(21): p. 7538-7550.

58. Bresnihan, B., et al., *Treatment of rheumatoid arthritis with recombinant human interleukin-1 receptor antagonist.* Arthritis & Rheumatism, 1998. **41**(12): p. 2196-2204.

59. Mertens, M. and J.A. Singh, *Anakinra for rheumatoid arthritis.* Cochrane Database Syst Rev, 2009. **1**.

60. Nuki, G., et al., *Long-term safety and maintenance of clinical improvement following treatment with anakinra (recombinant human interleukin-1 receptor antagonist) in patients with rheumatoid arthritis: Extension phase of a randomized, double-blind, placebo-controlled trial.* Arthritis & Rheumatism, 2002. **46**(11): p. 2838-2846.

61. Gundem, G., et al., *The evolutionary history of lethal metastatic prostate cancer.* Nature, 2015. **520**(7547): p. 353-357.

62. Hong, M.K.H., et al., *Tracking the origins and drivers of subclonal metastatic expansion in prostate cancer.* Nat Commun, 2015. **6**.

63. Penning, T.M., *Androgen biosynthesis in castration-resistant prostate cancer.* Endocrine-related cancer, 2014. **21**(4): p. T67-T78.

64. Shah, R.B., et al., *Androgen-independent prostate cancer is a heterogeneous group of diseases lessons from a rapid autopsy program.* Cancer research, 2004. **64**(24): p. 9209-9216.

65. Crnalic, S., et al., *Nuclear androgen receptor staining in bone metastases is related to a poor outcome in prostate cancer patients.* Endocrine-related cancer, 2010. **17**(4): p. 885-895.

66. Li, Z.G., et al., *Androgen receptor–negative human prostate cancer cells induce osteogenesis in mice through FGF9-mediated mechanisms.* The Journal of clinical investigation, 2008. **118**(8): p. 2697-2710.

67. Kim, D., et al., *Immunohistochemical quantitation of androgen receptor expression using color video image analysis.* Cytometry, 1999. **35**(1): p. 2-10.

68. Sheridan, T., et al., *The role of P501S and PSA in the diagnosis of metastatic adenocarcinoma of the prostate.* The American journal of surgical pathology, 2007. **31**(9): p. 1351-1355.

69. Cordon-Cardo, C., et al., *Improved prediction of prostate cancer recurrence through systems pathology.* The Journal of clinical investigation, 2007. **117**(7): p. 1876-1883.

70. Miyamoto, D.T., et al., *Androgen receptor signaling in circulating tumor cells as a marker of hormonally responsive prostate cancer.* Cancer discovery, 2012. **2**(11): p. 995-1003.

71. Aparicio, A., C.J. Logothetis, and S.N. Maity, *Understanding the lethal variant of prostate cancer: power of examining extremes.* Cancer discovery, 2011. **1**(6): p. 466-468.

72. Tan, H.-L., et al., *Rb loss is characteristic of prostatic small cell neuroendocrine carcinoma.* Clinical Cancer Research, 2014. **20**(4): p. 890-903.

73. Shariff, A.H. and M.H. Ather, *Neuroendocrine differentiation in prostate cancer.* Urology, 2006. **68**(1): p. 2-8.

74. Jiborn, T., A. Bjartell, and P.-A. Abrahamsson, *Neuroendocrine differentiation in prostatic carcinoma during hormonal treatment.* Urology, 1998. **51**(4): p. 585-589.

75. Sun, Y., J. Niu, and J. Huang, *Neuroendocrine differentiation in prostate cancer.* Am J Transl Res, 2009. **1**(2): p. 148-162.

76. Burrell, R.A., et al., *The causes and consequences of genetic heterogeneity in cancer evolution.* Nature, 2013. **501**(7467): p. 338-345.

77. Hong, M.K., et al., *Tracking the origins and drivers of subclonal metastatic expansion in prostate cancer.* Nature communications, 2015. **6**.

78. Weckermann, D., et al., *Disseminated cytokeratin positive tumor cells in the bone marrow of patients with prostate cancer: detection and prognostic value.* The Journal of urology, 2001. **166**(2): p. 699-703.

79. Xu, J., et al., *Identification and characterization of prostein, a novel prostate-specific protein.* Cancer research, 2001. **61**(4): p. 1563-1568.

80. Kalos, M., et al., *Prostein expression is highly restricted to normal and malignant prostate tissues.* The Prostate, 2004. **60**(3): p. 246-256.

81. Cindolo, L., et al., *NeuroD1 expression in human prostate cancer: can it contribute to neuroendocrine differentiation comprehension?* European urology, 2007. **52**(5): p. 1365-1373.

82. Komiya, A., et al., *Neuroendocrine differentiation in the progression of prostate cancer.* International Journal of Urology, 2009. **16**(1): p. 37-44.

83. Beltran, H., et al., *Molecular characterization of neuroendocrine prostate cancer and identification of new drug targets.* Cancer discovery, 2011. **1**(6): p. 487-495.

84. Chang, M., et al., *IL-1β Induces p62/SQSTM1 and Represses Androgen Receptor Expression in Prostate Cancer Cells.* Journal of cellular biochemistry, 2014. **115**(12): p. 2188-2197.

85. Culig, Z., et al., *Interleukin 1beta mediates the modulatory effects of monocytes on LNCaP human prostate cancer cells.* British journal of cancer, 1998. **78**(8): p. 1004.

86. Drake, J.M., C.L. Gabriel, and M.D. Henry, *Assessing tumor growth and distribution in a model of prostate cancer metastasis using bioluminescence imaging.* Clinical & experimental metastasis, 2005. **22**(8): p. 674-684.

87. Drake, J.M., J.R. Danke, and M. Henry, *Bone-specific growth inhibition of prostate cancer metastasis by atrasentan.* Cancer biology & therapy, 2010. **9**(8): p. 607-614.

88. Bersani, F., et al., *Bioengineered implantable scaffolds as a tool to study stromal-derived factors in metastatic cancer models.* Cancer research, 2014. **74**(24): p. 7229-7238.

89. Klein, C.A., *Selection and adaptation during metastatic cancer progression.* Nature, 2013. **501**(7467): p. 365-372.

90. Bedard, P.L., et al., *Tumour heterogeneity in the clinic.* Nature, 2013. **501**(7467): p. 355-364.

91. Kapanci, Y., et al., *Cytoskeletal features of alveolar myofibroblasts and pericytes in normal human and rat lung.* Journal of Histochemistry & Cytochemistry, 1992. **40**(12): p. 1955-1963.

92. Paget, S., *The distribution of secondary growths in cancer of the breast.* The Lancet, 1889. **1**(3421): p. 571-573.

93. Kalluri, R. and M. Zeisberg, *Fibroblasts in cancer.* Nature Reviews Cancer, 2006. **6**(5): p. 392-401.

94. Polanska, U.M. and A. Orimo, *Carcinoma-associated fibroblasts: Non-neoplastic tumour-promoting mesenchymal cells.* Journal of cellular physiology, 2013. **228**(8): p. 1651-1657.

95. Sugimoto, H., et al., *Identification of fibroblast heterogeneity in the tumor microenvironment.* Cancer biology & therapy, 2006. **5**(12): p. 1640-1646.

96. van den Hoogen, C., et al., *High aldehyde dehydrogenase activity identifies tumor-initiating and metastasis-initiating cells in human prostate cancer.* Cancer research, 2010. **70**(12): p. 5163-5173.

97. Madar, S., I. Goldstein, and V. Rotter, *'Cancer associated fibroblasts'–more than meets the eye.* Trends in molecular medicine, 2013. **19**(8): p. 447-453.

98. Orimo, A., et al., *Stromal fibroblasts present in invasive human breast carcinomas promote tumor growth and angiogenesis through elevated SDF-1/CXCL12 secretion.* Cell, 2005. **121**(3): p. 335-348.

99. Giannoni, E., et al., *Reciprocal activation of prostate cancer cells and cancer-associated fibroblasts stimulates epithelial-mesenchymal transition and cancer stemness.* Cancer research, 2010. **70**(17): p. 6945-6956.

100. Karagiannis, G.S., et al., *Cancer-associated fibroblasts drive the progression of metastasis through both paracrine and mechanical pressure on cancer tissue.* Molecular Cancer Research, 2012. **10**(11): p. 1403-1418.

101. Garrett, S.C., et al., *S100A4, a mediator of metastasis.* Journal of Biological Chemistry, 2006. **281**(2): p. 677-680.

102. Goel, H.L., et al., *Integrins in prostate cancer progression.* Endocrine-related cancer, 2008. **15**(3): p. 657-664.

103. Hemingway, F., et al., *RANKL-independent human osteoclast formation with APRIL, BAFF, NGF, IGF I and IGF II.* Bone, 2011. **48**(4): p. 938-944.

104. Wai, P.Y. and P.C. Kuo, *Osteopontin: regulation in tumor metastasis.* Cancer and Metastasis Reviews, 2008. **27**(1): p. 103-118.

105. Yu, D., et al., *ILs-3, 6 and 11 increase, but ILs-10 and 24 decrease stemness of human prostate cancer cells in vitro.* Oncotarget, 2015. **6**(40): p. 42687.

106. Pio, R., L. Corrales, and J.D. Lambris, *The role of complement in tumor growth*, in *Tumor microenvironment and cellular stress*. 2014, Springer. p. 229-262.

107. Kim, S., et al., *In vivo natural killer cell activities revealed by natural killer cell-deficient mice.* Proceedings of the National Academy of Sciences, 2000. **97**(6): p. 2731-2736.

108. Childs, R.W. and M. Carlsten, *Therapeutic approaches to enhance natural killer cell cytotoxicity against cancer: the force awakens.* Nature reviews Drug discovery, 2015. **14**(7): p. 487-498.

109. Knudsen, K.E. and T.M. Penning, *Partners in crime: deregulation of AR activity and androgen synthesis in prostate cancer.* Trends in Endocrinology & Metabolism, 2010. **21**(5): p. 315-324.

110. Armstrong, A.J., et al., *The development of risk groups in men with metastatic castration-resistant prostate cancer based on risk factors for PSA decline and survival.* European journal of cancer, 2010. **46**(3): p. 517-525.

111. Xu, L., et al., *COX-2 inhibition potentiates antiangiogenic cancer therapy and prevents metastasis in preclinical models.* Science translational medicine, 2014. **6**(242): p. 242ra84-242ra84.